



## Investigation of the accelerated corrosion of cupro-nickel piping

|               |   |
|---------------|---|
| Title         | Investigation of the accelerated corrosion of cupro-nickel piping                   |
| Item Type     | Thesis  |
| Authors       | Brown, Martin Richard   |
| URI           | <a href="https://hdl.handle.net/10945/18769">https://hdl.handle.net/10945/18769</a> |
| Publisher     | Massachusetts Institute of Technology   |
| Date Issued   | 1979-06   |
| Download date | 2026-04-14 23:22:13   |
| Link to Item  | <a href="https://hdl.handle.net/10945/18769">https://hdl.handle.net/10945/18769</a> |

**Downloaded from NPS Archive: Calhoun**



DUDLEY KNOX LIBRARY  
NAVAL POSTGRADUATE SCHOOL  
MONTEREY, CALIF 93940

T197803







## REPORT DOCUMENTATION PAGE

READ INSTRUCTIONS  
BEFORE COMPLETING FORM

|  |                       |  |
|--|-----------------------|--|
| 1. REPORT NUMBER   | 2. GOVT ACCESSION NO. | 3. RECIPIENT'S CATALOG NUMBER                                  |
| 4. TITLE (and Subtitle)<br>Investigation of the Accelerated Corrosion of<br>Cupro-Nickel Piping  |                       | 5. TYPE OF REPORT & PERIOD COVERED<br>THESIS                   |
| 7. AUTHOR(s)<br>Brown, Jr., Martin R.  |                       | 8. PERFORMING ORG. REPORT NUMBER                               |
| 9. PERFORMING ORGANIZATION NAME AND ADDRESS<br>Massachusetts Institute of Technology<br>Cambridge, Massachusetts                                 |                       | 8. CONTRACT OR GRANT NUMBER(s)                                 |
| 11. CONTROLLING OFFICE NAME AND ADDRESS<br>CODE 031<br>NAVAL POSTGRADUATE SCHOOL<br>MONTEREY, CALIFORNIA 93940                                   |                       | 10. PROGRAM ELEMENT, PROJECT, TASK<br>AREA & WORK UNIT NUMBERS |
| 11. CONTROLLING OFFICE NAME AND ADDRESS  |                       | 12. REPORT DATE<br>June 1979                                   |
| 11. CONTROLLING OFFICE NAME AND ADDRESS  |                       | 13. NUMBER OF PAGES<br>83                                      |
| 14. MONITORING AGENCY NAME & ADDRESS (if different from Controlling Office)  |                       | 15. SECURITY CLASS (of this report)<br>UNCLASS                 |
| 14. MONITORING AGENCY NAME & ADDRESS (if different from Controlling Office)  |                       | 15a. DECLASSIFICATION/DOWNGRADING<br>SCHEDULE                  |
| 16. DISTRIBUTION STATEMENT (of this Report)<br><br>APPROVED FOR PUBLIC RELEASE; DISTRIBUTION UNLIMITED   |                       |  |
| 17. DISTRIBUTION STATEMENT (of the abstract entered in Block 20, if different from Report)   |                       |  |
| 18. SUPPLEMENTARY NOTES  |                       |  |
| 19. KEY WORDS (Continue on reverse side if necessary and identify by block number)<br>Water Pollution<br>Marine Engineering<br>Corrosion Science |                       |  |
| 20. ABSTRACT (Continue on reverse side if necessary and identify by block number)<br><br>SEE REVERSE   |                       |  |

## ABSTRACT

The accelerated corrosion (erosion) of 70/30 cupro-nickel alloy was investigated as a function of environment using a laboratory recirculation loop. The environments utilized were unpolluted artificial sea water and artificial sea water polluted with sulfides ( $\text{Na}_2\text{S}$ ) and two different levels of ammonium ion ( $\text{NH}_4\text{Cl}$ ). The use of ferrous sulfate ( $\text{FeSO}_4$ ) as an inhibitor was also briefly examined. The results indicated that  $\text{S}^-$  and  $\text{NH}_4^+$  acting synergistically increased the amount of localized corrosion observed, and the higher level of  $\text{NH}_4^+$  in conjunction with  $\text{S}^-$  was even more detrimental, compared to the amount of localized corrosion observed due to  $\text{S}^-$  acting alone. Ferrous sulfate treatment of the polluted environment on an intermittent basis reduced the amount of pitting observed, but did not prevent it. Samples were examined visually and microscopically, and surface films identified by use of Energy Dispersive X-Ray Analysis. Micrographs are included and a discussion of possible mechanisms presented.

INVESTIGATION OF  
THE ACCELERATED CORROSION OF CUPRO-NICKEL PIPING

by

MARTIN RICHARD BROWN, JR.

B.S., University of Oklahoma  
(1972)

SUBMITTED IN PARTIAL FULFILLMENT  
OF THE REQUIREMENTS FOR THE  
DEGREES OF

OCEAN ENGINEER

and

MASTER OF SCIENCE IN  
NAVAL ARCHITECTURE AND MARINE ENGINEERING

at the

MASSACHUSETTS INSTITUTE OF TECHNOLOGY

JUNE 1979

© MARTIN RICHARD BROWN, JR. 1979



INVESTIGATION OF  
THE ACCELERATED CORROSION OF CUPRO-NICKEL PIPING

by

MARTIN RICHARD BROWN, JR.

Submitted to the Department of Ocean Engineering on May 11, 1979 in partial fulfillment of the requirements for the Degrees of Ocean Engineer and Master of Science in Naval Architecture and Marine Engineering.

ABSTRACT

The accelerated corrosion (erosion) of 70/30 cupro-nickel alloy was investigated as a function of environment using a laboratory recirculation loop. The environments utilized were unpolluted artificial sea water and artificial sea water polluted with sulfides ( $\text{Na}_2\text{S}$ ) and two different levels of ammonium ion ( $\text{NH}_4\text{Cl}$ ). The use of ferrous sulfate ( $\text{FeSO}_4$ ) as an inhibitor was also briefly examined. The results indicated that  $\text{S}^{=}$  and  $\text{NH}_4^+$  acting synergistically increased the amount of localized corrosion observed, and the higher level of  $\text{NH}_4^+$  in conjunction with  $\text{S}^{=}$  was even more detrimental, compared to the amount of localized corrosion observed due to  $\text{S}^{=}$  acting alone. Ferrous sulfate treatment of the polluted environment on an intermittent basis reduced the amount of pitting observed, but



did not prevent it. Samples were examined visually and microscopically, and surface films identified by use of Energy Dispersive X-Ray Analysis. Micrographs are included and a discussion of possible mechanisms presented.

Name and Title of Thesis Supervisor: Ronald M. Latanision  
Associate Professor  
Mat. Sci. and Engr.



TABLE OF CONTENTS

|  | <u>Page</u> |
|--|-------------|
| TITLE PAGE.....                              | 1           |
| ABSTRACT.....                                | 2           |
| TABLE OF CONTENTS.....                       | 4           |
| LIST OF FIGURES.....                         | 5           |
| TERMINOLOGY.....                             | 8           |
| ACKNOWLEDGMENTS.....                         | 11          |
| CHAPTER I. INTRODUCTION.....                 | 12          |
| A. Motivation.....                           | 12          |
| B. Problem Statement.....                    | 20          |
| CHAPTER II. BACKGROUND.....                  | 22          |
| A. Theory of Corrosion Resistance.....       | 22          |
| CHAPTER III. MATERIALS AND TEST METHODS..... | 36          |
| A. Experimental Methods.....                 | 36          |
| B. Materials.....                            | 38          |
| C. Test Equipment.....                       | 39          |
| D. Test Procedures.....                      | 40          |
| E. Sample Examination.....                   | 43          |
| CHAPTER IV. RESULTS AND DISCUSSION.....      | 45          |
| A. Results.....                              | 45          |
| B. Discussion.....                           | 54          |
| C. Conclusion.....                           | 60          |
| REFERENCES.....                              | 62          |
| FIGURES.....                                 | 67          |



LIST OF FIGURES

|           |  | <u>Page</u> |
|-----------|--|-------------|
| Figure 1  | Schematic of Changes in the Erosion-Corrosion Mechanism as Velocity is Increased           | 67          |
| Figure 2  | Erosion-Corrosion as a Function of Velocity and Temperature                                | 68          |
| Figure 3  | Schematic of an "Undoped" $\text{Cu}_2\text{O}$ Cation Lattice                             | 69          |
| Figure 4  | Schematic of Recirculation Loop  | 70          |
| Figure 5  | Schematic of Short-Pipe Orifice  | 71          |
| Figure 6  | Pressure versus Velocity for Short-Pipe Orifice  | 72          |
| Figure 7  | Experimental Potential and PH Values   | 73          |
| Figure 8  | Sample Exposed to Salt Water   | 74          |
| Figure 9  | Sample Exposed to Salt Water + Low Ammonia   | 74          |
| Figure 10 | Sample Exposed to Salt Water + Low Ammonia + Sulfide                                       | 74          |
| Figure 11 | Sample Exposed to Salt Water + Sulfide   | 75          |
| Figure 12 | Sample Exposed to Salt Water + High Ammonia  | 75          |
| Figure 13 | Dark, Flaky Film on Sample Exposed to Salt Water + High Ammonia + Sulfide at 40X           | 75          |
| Figure 14 | Sample Exposed to Salt Water + High Ammonia + Sulfide with Dark, Flaky Film Removed at 40X | 76          |



|           | <u>Page</u>   |    |
|-----------|---|----|
| Figure 15 | Sample Exposed to Salt Water +<br>High Ammonia + Sulfide  | 76 |
| Figure 16 | Sample Exposed to Salt Water +<br>High Ammonia + Sulfide + Ferrous<br>Sulfate   | 76 |
| Figure 17 | Representative Pit from Sample<br>Exposed to Salt Water + Sulfide<br>at 40X   | 77 |
| Figure 18 | Sample Exposed to Salt Water +<br>Sulfide Showing Transition From<br>the Light to the Dark Area and a<br>Corrosion Pit at 40X           | 77 |
| Figure 19 | Sample Exposed to Salt Water +<br>Sulfide Showing the Powder-Like<br>Nature of the Dark Film at 1000X                                   | 77 |
| Figure 20 | EDAX Scan of the Dark Film on the<br>Sample Exposed to Salt Water +<br>Sulfide  | 78 |
| Figure 21 | Corrosion Pit from Sample Exposed<br>to Salt Water + Sulfide at 100X  | 78 |
| Figure 22 | Corrosion Pit Three-Way Junction<br>Between the Inner Pit Base Metal,<br>the Corrosion Product, and the<br>Thin Corrosion Film at 1000X | 79 |
| Figure 23 | Dark, Flaky Film from Sample Exposed<br>to Salt Water + High Ammonia +<br>Sulfide at 100X   | 79 |
| Figure 24 | Auger Line Scan of Sulfur Passing<br>Between Light and Dark Areas of<br>Sample Exposed to Salt Water +<br>Sulfide                       | 79 |
| Figure 25 | Auger Line Scan of Copper Inside of<br>a Corrosion Pit  | 80 |
| Figure 26 | Auger Line Scan of Nickel Inside of<br>a Corrosion Pit  | 80 |



|           |  | <u>Page</u> |
|-----------|--|-------------|
| Figure 27 | Pourbaix Diagram for Pure Copper   | 81          |
| Figure 28 | Experimental Potential - PH<br>Diagram for 70/30 Cupronickel             | 82          |
| Figure 29 | Schematic of the Erosion-Corrosion<br>Process in the Presence of Ammonia | 83          |



## TERMINOLOGY

Accelerated Corrosion - term used primarily in reference to the enhanced corrosion of cupro-nickel alloys in polluted sea water environments, specifically those polluted with sulfides and considered to involve the combined action of fluid flow and electrochemical corrosion.

Alloy 706 - cupro-nickel alloy containing 90% copper and 10% nickel.

Alloy 715 - cupro-nickel alloy containing 70% copper and 30% nickel.

Angstrom - unit of length of value  $1.0 \times 10^{-8}$  cm.

Anoxic - term meaning oxygen-free conditions in sea water.

Breakaway Velocity - the velocity of fluid over the surface of cupro-nickel alloys below which accelerated corrosion does not occur.

Corrosion Potential - the measured potential of a corroding metal; the compromise potential of both polarized anodes and cathodes.

Design Velocity - refers to the velocity value used in design to prevent accelerated corrosion and in essence is the same as the breakaway velocity.



Electronic Conductance - property of a material which places a relative value on the ease with which electrons pass through the material.

Electrophoresis - phenomenon of migration of suspended particles, liquid or solid, through a fluid, gaseous or liquid, as a result of the imposition of an electric field between electrodes immersed in the fluid.

Erosion-Corrosion - combined effects of erosion and corrosion whereby the shear force exerted by the flowing liquid becomes sufficiently high to cause effective removal of corrosion products in localized areas.

Inhibitor - a chemical substance that, when added in small concentration to an environment, effectively decreases the corrosion rate.

Ionic Conductance - property of a material which places a relative value on the ease with which ions pass through the material.

M-Bronze - manganese bronze.

PPM - parts per million by weight.

p-Type Semiconductor - impurity atoms having only three valence electrons are fit into the crystal with four bonds on each atom. Therefore, each impurity atom is prepared



to accept a free electron or supply one hole. Since no extra free electrons are introduced, holes become the majority carrier, far outnumbering the thermally generated free electrons still present.

Putrefaction - decomposition of organic matter.



ACKNOWLEDGEMENTS

I would like to express my gratitude to the following people: to my lovely wife, Margaret, for her support throughout the term of this project; to Professor Ronald Latanision for his advice, counsel, and financial aid; and to Mr. George Danek of NSRDC, Annapolis for his technical and logistic support. I sincerely hope that my effort here does not seriously disappoint any of you.



## CHAPTER 1

IntroductionA. Motivation

Copper and its alloys have long been utilized in marine environments for a variety of reasons. One important property is resistance to fouling by marine organisms. Copper and many of its alloys have the ability to suppress attachment of marine animals, possibly due to the toxic effects of the corrosion products or copper ions released as part of the corrosion process (1). Fouling resistance alone makes copper alloys attractive as materials of construction for marine applications. However, corrosion resistance is another very important factor. The good service of copper alloys in marine applications is due partly to their inherent chemical stability, but is largely due to their ability to form films of corrosion products that are resistant to erosion by turbulently flowing sea water. For these reasons, copper alloys, depending on alloy composition, can vary considerably in corrosion performance. Cupro-nickel 30% - 715 has a higher resistance to sea water corrosion than most condenser tube alloys and is widely used in naval vessels (2).

The marine environment can vary considerably depending on location and whether or not exposure is in sea water or in a marine atmosphere. In addition, pollutants and tempera-



ture play an important role. Pollutants such as sulfides and ammonia are often present in coastal estuaries, and play a vital role in the overall corrosion resistance of copper alloys. Accelerated corrosion of cupro-nickel alloys in a polluted sea water environment has been recognized for some time. Although a considerable amount of work has been reported on this topic, no completely acceptable mechanism for the accelerated attack has been formulated (3). One difficulty associated with the accelerated corrosion mechanism is the very low concentrations of pollutants involved. It has been observed that sulfide contents in the order of 1-2 ppm may be sufficient to considerably accelerate corrosion (1). Another complicating factor is that  $\text{NH}_3$  is often present in polluted sea water as a result of sewage discharge or decay of marine organic material. Ammonia is known to have a detrimental effect on the general corrosion resistance of copper base alloys, but its effect on the accelerated corrosion behavior of cupro-nickel alloys is relatively unknown. In addition, the pH of sea water can vary widely, although at the normal pH of sea water (8.1 to 8.3), the general corrosion rates are extremely low.

Some of the most common uses of copper base alloys in marine service are as condenser tubes or salt water circulating pipes in power generating plants and ships. In general, cupro-nickel alloys are much superior to other alloy systems



in these applications. However, when the sea water becomes polluted, that may not be the case. An industrial survey of prior corrosion experience with alloy 706 in sea water piping systems resulted in the following (4):

1. Most cases of corrosion of cupro-nickel pipe are caused by pollution, deposits, or a combination of these factors.
2. Methods for alleviating the problem consist of the use of ferrous sulfate as a corrosion inhibitor, flushing systems with clean fresh water, and maintaining cleanliness.
3. Sulfide causing the corrosion of cupro-nickel pipes may not be present in an amount sufficient to be detectable by the usual analytical methods.

This industrial experience survey was conducted by the Naval Ship Research and Development Center (NSRDC), Annapolis Laboratory. The same group conducted a similar survey of Naval experience with alloy 706 (4). It was found that the problem of serious accelerated corrosion surfaced in March, 1974, at an East Coast shipyard. A Navy ship was built and remained dockside in the fitting out basin for a period of approximately 2-1/2 years. During this time, the piping systems were filled with basin water and exposed intermittently to both flowing and stagnant conditions. Corrosion of the alloy 706 piping was found to occur in the form of sharp



edged pits of varying sizes and depths. No attack was observed on M-bronze fittings in the systems although the cupro-nickel alloy adjacent to the bronze components was pitted. Some of the corroded pipe was replaced in April, 1974, after which the ship went to sea. Examination of the pipe in September, 1974, showed that corrosion had not recurred.

Laboratory and field measurements taken by NSRDC in the fitting out basin and nearby waterways led to the following conclusions (5):

1. There was no significant level of sulfide concentration in the water in question. If sulfide existed, it was in quantities at or below present detection levels of the methods of chemical analysis.
2. There was no indication of any large scale catastrophic environmental changes that could cause the corrosion to be initiated by a one time effect, including chemical dumps.
3. There have been detected no corrosive organic chemicals.
4. There were no industries near the shipyard which introduced harmful chemicals that could cause the cupro-nickel corrosion.
5. There was no significant level of heavy metals found in the water.



6. Bacteria capable of producing sulfide (under proper conditions) have been found in the water at several locations and in the bottom sediment.
7. A high level of nitrogen compounds, particularly ammonia, was found to be present in the water.
8. The sewage treatment plants above and below the shipyard contributed to the high concentrations of nitrogen compounds in the water. The shipyard contribution of these compounds was small.
9. The shipyard contributed, according to their records, 27 pounds of sulfide per day into the water.

The above listed conclusions give some insight into the origin of accelerated corrosion experienced by Navy ships. Another notable source of rapid failure in some cases has been dredging in the vicinity of the ship. Dredging of the bottom sediment would naturally reintroduce pollutants that had settled out back into the basin water.

The evidence presented thus far indicates that when once a good protective film has been formed on the tubes or piping by normal working in the open sea, there is a better chance of resisting the effects of pollution. If, however, polluted waters are encountered during the early life, the films or corrosion products formed will likely not be fully protective and the risk of premature failure is considerably increased (6).



Other aspects of the corrosion problem have been investigated by NSRDC. It was found that the materials employed, operating parameters, and fabrication parameters were not causing the attack (7). No spacial, geometric, or location dependence was discovered in the affected systems (8). The following observations were made from a visual inspection of the corrosion discovered on a Navy ship in March, 1974 (8):

1. Only the 706 alloy was attacked. M-bronze fittings were free from accelerated attack.
2. Where detected, pitting predominantly occurred within a few inches downstream of flanges, elbows, or other fittings that caused turbulence. Pitting very rarely occurred upstream of elbows or flanges.
3. The regions attacked generally displayed films which differed in appearance from the normal, dark brown, tightly adherent cuprous-oxide film. Many pits were coated with loose black or brown film. Furthermore, pitted components usually had loose, flaky films of various colors, including green, black, and sometimes red.
4. The appearance of the pits was that of regularly shaped craters of varying depth.

Another major complicating factor in accelerated corrosion is the effect of velocity of flow. The location of attacked regions in the piping system and the appearance

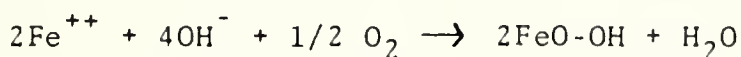


strongly suggest that turbulence is a major factor contributing to aggressive attack, and in fact actually increases corrosion. Actual service observations indicate that severe attack occurs at higher velocities (greater than 8 ft/sec) but not at lower velocities (6 ft/sec). Moreover, it is recognized that these test results are contradictory to established data and commercial experience for cupro-nickel alloys in sulfide environments (9). An overall, critical review of the observations presented suggests that high velocity coupled with the environment of polluted sea water is the main cause of the rapid corrosion observed.

Based on the observations made, an acceptable method of preventing accelerated corrosion would be to ensure the establishment of a strongly adherent oxide film on the pipe or tube surface. Navy tests have shown that alloy 706 piping pre-exposed 120 days to uncontaminated sea water developed a sufficiently protective film to avoid attack of the type being discussed here (9). Unfortunately, the kinetics of this prefilming process are too slow to be economically feasible. Another possibility would be the use of corrosion inhibitors. The two corrosion inhibitors which appear to be used frequently are ferrous sulfate and sodium dimethyl dithiocarbamate. The use of ferrous sulfate appears to be almost standard practice when aluminum brass tubing or pipe is in use (6). There has been some difference of opinion about its



effectiveness with the cupro-nickel alloys, but recent data published by Cohen and George (10) show that the corrosion of 706 cupro-nickel was cut approximately in half when ferrous sulfate treatment was employed. Another method of inhibition consists of installing steel pieces in an upstream location so that they are free to corrode. The steel pieces become, in essence, sacrificial anodes. Whatever the method of introduction, the ferrous ion reduces corrosion of cupro-nickels both by improving the protectiveness of the corrosion product films and by removing sulfide ions from the water by precipitation as FeS (9). The mechanism by which the protectiveness of the corrosion product film is improved (6) involves the deposition of a brown layer of lepidocrocite ( $\gamma$  FeO-OH) on the cathodic areas of the metal surface. This increases the polarization of the cathodic reaction which is believed to be the reduction of dissolved oxygen. Ferrous ions in solution are oxidized directly to lepidocrocite as follows:



The lepidocrocite is then carried electrophoretically to the cathode areas. While ferrous ions are known to scavenge sulfide ions from sea water, the influence of ferrous ions on ammonia compounds is not known. Information is also lacking on combinations of sulfides and ammoniacal contaminants in sea water.



## B. Problem Statement

The accelerated corrosion of cupro-nickel piping in polluted sea water (specifically polluted with sulfides) has been studied extensively. It should be noted that, in most cases, a deaerated solution was used, due to the complication that oxygen reacts with sulfides forming stable ions, thus, in effect, preventing their reaction with the metal in question. The interest here centers on the combined effect of oxygen and sulfides. Other areas of concentration will be the effect of ammonia alone, and in combination with oxygen and sulfides. A feel for the synergistic effect of ammonia and sulfide is a primary goal.

The effect of ammonia on the accelerated corrosion mechanism is an area that has not been investigated thoroughly. Ammonia is known to be detrimental in concentrations as low as 10 ppm. However, its effect in combination with sulfides is relatively unknown.

Levels of total sulfide in natural waters range from less than 1 to 30 ppm. The Naval Research Lab conducted a study of polluted harbors in 1960 and found total sulfide varying intermittently around 1 ppm, and it may be higher now (11). Campbell states, "The addition of 10 ppm of hydrogen sulfide in seawater each working day gives conditions probably comparable with the most severe that might be encountered in service on account of pollution" (12). It must



be remembered that the presence of either sulfide plus low oxygen or oxygen alone leads to low corrosion rates. However, when both sulfide and oxygen are present in certain concentration ranges, dramatic increases in the corrosion rate result (13).

In summary, the areas discussed above will be the areas of concentration. In addition, the effect of ferrous sulfate as an inhibitor will also be briefly examined.



## CHAPTER 2

BackgroundA. Theory of Corrosion Resistance

In the present context, accelerated corrosion is a combined effect of erosion and corrosion. This phenomenon, erosion-corrosion, is fairly well understood. Ignoring the effect of abrasives such as sand or silt, at certain critical velocities, the shear force exerted by the flowing liquid becomes sufficiently high to cause effective removal of corrosion products in localized areas. The corrosion rate in these areas is then accelerated by galvanic action under the adverse conditions of a small anode (the area which is film-free) and large cathode (the remaining metal surface with its corrosion product intact). Naturally the fluid dynamics play a complex and important role in erosion-corrosion. In particular, the critical surface shear stress is dependent on many factors, described in a recent paper by Efird (14). Here, however, the bulk flow rate velocity, which in some cases can be related to shear force, will be used. It must be noted, however, that erosion-corrosion as related to bulk flow rate is only an approximation, since geometric effects play an important role.



Design velocities below which erosion-corrosion is not a problem have been established for both alloy 706 and alloy 715. For instance, the design velocity for alloy 706 is typically 5 to 7 ft/sec for 1 inch diameter tubes. It has been reported that alloy 715 has a design velocity of about 16.4 ft/sec when sea water flows through smooth pipes, but that this drops to about 9.8 ft/sec when the degree of turbulence is increased (15). These "design velocities" will hereafter be referred to as the "breakaway" velocity. Not all metals exhibit a breakaway velocity. Danek (16) exposed 53 alloys, including stainless steels and alloys of titanium, nickel, and copper, to sea water flowing at velocities in the range of 0 to 120 ft/sec. He found that the alloys fell into three groups according to their film-forming characteristics, and each group responded differently to sea water velocity. Alloys in the first group form very tenacious and protective surface oxide films and have excellent corrosion resistance at all velocities: titanium alloys and one Ni-Cr-Mo alloy were in this category. Alloys in the second group also form very protective surface films and exhibit excellent corrosion resistance at high and intermediate velocities. However, at low velocities, where the settling of sand and other deposits is possible, pitting and crevice corrosion is often a problem. Most stainless steels and nickel alloys were in this category. Alloys in the third group exhibit excellent corrosion resis-



tance at low velocities but are subject to degradation by erosion-corrosion in the high and intermediate range; at the latter velocities, the protective oxide films are thought to be stripped from the metal surface. Copper-based alloys were in this category. As can be seen, the metal system and fluid dynamics play a vital role in the erosion-corrosion characteristics exhibited. Looking for a moment at a general case (category 3) in which erosion-corrosion increases with velocity, a schematic of 5 different zones in the corrosion process as a function of velocity can be visualized (see Figure 1) (15). Depending on the precise alloy and environment, each zone may be narrower or wider than that shown in Figure 1, or may be completely absent. In addition, the boundary between adjacent zones may not occur at one velocity but rather over a range of velocities. The corrosion and erosion processes characteristic of each zone are discussed below, starting with zone A at low velocities and ending with zone E at high velocities.

ZONE A (Rarely Encountered Under Service Conditions)

1. There is a relatively poor oxygen supply, but the oxide (or other surface film) is protective.
2. Water flow is laminar. Shear stresses are not sufficiently large to disrupt the oxide film.



ZONE B

1. Flow is now turbulent (or unstable turbulent/laminar), but the oxide is still protective.

ZONE C

1. The degree of turbulence and the shear stresses are so great that oxide is removed from the underlying metal surface in a few areas.
2. Attack of the exposed areas is severe. The problem is compounded by galvanic currents flowing between the metal (anodic) and the oxide (cathodic).
3. If the repassivation kinetics allow it, the corroding pit-shaped areas will eventually heal, and attack will initiate in other areas.

ZONE D

1. The oxide removal is more general, so the contribution to corrosion from the galvanic current between oxide and metal is reduced.
2. The degree of turbulence and shear stresses are greatly increased. Repassivation is very difficult.

ZONE E

1. Oxide removal is complete and repassivation is essentially impossible.



It seems likely that the breakaway velocity coincides with the initial breakdown of the protective oxide film by mechanical, chemical, or electrochemical processes. Unfortunately, few, if any, data are now available that indicate the relative contributions of erosion and corrosion at velocities greater than the breakaway velocity (15).

Several other variables have a significant effect on the erosion-corrosion process, specifically pH, oxygen, and temperature. Lowering the pH of sea water increases the rate of erosion-corrosion. On the other hand, corrosion of copper alloys is either eliminated or greatly reduced when the sea water has been deaerated. There is apparent disagreement in the reported effects of temperature, undoubtedly due in part to the variations in the oxygen content of the waters tested. While reaction kinetics and oxygen diffusivity are expected to increase as the temperature increases, the solubility of oxygen in the water will decrease. In addition, the character of the surface film may change as the temperature is increased because of thermodynamic considerations. When it is also considered that oxygen solubility is a function of the chloride content of the water, and that the kinetics of repassivation are a function not only of temperature but also of alloy composition, water velocity, and chloride content of the water, it is not surprising that the reported effects of temperature are so variable (15). In sea



water that has been deaerated, a much clearer picture emerges of the corrosion behavior of copper alloys exposed to a variety of temperature and velocity conditions. Based on the results of many studies, Anderson (17) has summarized his findings in terms of a velocity versus temperature diagram (Figure 2). Three distinct zones are indicated: (1) Zone A, generally representing the lower temperatures and higher velocities, where erosion-corrosion becomes a dominating factor; (2) Zone B, a transition zone where erosion-corrosion can occur, but generally develops to a less significant extent; and (3) Zone C, where corrosion of all types is minimal and the more corrosion resistant alloys can provide virtual immunity to erosion-corrosion.

From the above discussion, it is obvious that the characteristics of the film initially formed are extremely important. Copper base alloys are somewhat unique in that they do not form a corrosion product film which in the classical sense is "passive" (1). In salt water or sea water, the corrosion product is predominately  $\text{Cu}_2\text{O}$  (cuprous oxide) irrespective of alloy composition (18,19). In polluted sulfide containing environments,  $\text{Cu}_2\text{S}$  may be formed (20,21). Other corrosion products may include  $\text{Cu}(\text{OH})_2$ ,  $\text{CuO}$ ,  $\text{CuCl}_2$ , and  $\text{Cu}_3(\text{OH})_2(\text{CO}_3)_2$  (22). However, in the majority of cases,  $\text{Cu}_2\text{O}$  is the corrosion product responsible for corrosion protection and its properties therefore are extremely important.

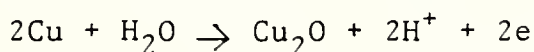


North and Pryor (18) have observed that corrosion rates decrease sharply with time in a parabolic manner in salt water, indicating that as the  $\text{Cu}_2\text{O}$  corrosion product film thickens, the corrosion rate decreases. All copper alloys show essentially the same behavior (i.e., high initial corrosion rates decreasing to a low steady state value after a period of time). However, depending on the alloy system, initial and steady state corrosion rates vary significantly. It is clear from recent studies that alloying additions such as zinc reduce corrosion rates and that nickel is even more effective. In all cases, however, the primary corrosion product is  $\text{Cu}_2\text{O}$ . The question is raised therefore as to why, if different alloys form the same corrosion product that vastly different corrosion rates are observed? Two explanations exist as detailed by Popplewell (1). Firstly, the more resistant alloys may form a thicker corrosion product film. It has been observed that the reverse in fact is normally true in that the more resistant alloys, such as the cupro-nickels, form steady state corrosion product films in the order of 500-5000 Angstroms in thickness in 3.4% NaCl solution; whereas, the less resistant brasses form corrosion products in excess of 8000 Angstroms in thickness. The alternative explanation is therefore that the electronic and ionic conductance of the corrosion product must in some way be altered by the presence of alloying additions. Work by

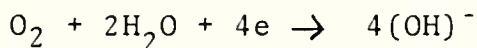


North and Pryor (18) and Popplewell has confirmed that alloying elements can become incorporated into the  $\text{Cu}_2\text{O}$  corrosion product film as "dopants" changing the defect structure. These alloying elements can only enter the oxide film and change the defect structure from solid solution in the substrate.

Cuprous oxide is a highly defective p-type semiconductor and is formed by the anodic reaction



The cathodic reaction is the reduction of oxygen



In order to corrode, copper ions and electrons must pass through the  $\text{Cu}_2\text{O}$  corrosion product. It is clear therefore that both ionic and electronic conductivity of the  $\text{Cu}_2\text{O}$  are highly important. A decrease in either of these quantities will significantly reduce corrosion rates, since anodic and cathodic reactions will be stifled. A linear relationship exists between corrosion rate and the reciprocal sum of the ionic and electronic resistance (18).

The "doping" effect is best understood by consideration of the cupro-nickel system. An "undoped" defective  $\text{Cu}_2\text{O}$  cation lattice is schematically illustrated in Figure 3. Cation vacancies exist permitting easy ionic diffusion. In addition, to ensure electrical neutrality, a local valency change to  $\text{Cu}^{2+}$  is necessary (i.e., the vacancy can be imagined



to carry a positive charge) permitting easy movement of electrons by a valency change mechanism. The  $\text{Ni}^{2+}$  ion can be incorporated into the defective  $\text{Cu}_2\text{O}$  lattice by either occupying a cation vacancy or by substitution for  $\text{Cu}^+$ . In the first case, an increase in both ionic and electronic resistivity due to a net reduction in the number of cation vacancies and the necessary addition of electrons to achieve charge neutrality would occur. In the second case, no increase in ionic resistivity is possible and only electronic resistivity would increase. As the number of valence electrons increases, the net increase in electronic resistivity would be expected to increase. This has in fact been observed for iron as an addition to cupro-nickel (19).

At the current time, it is not clearly understood why certain elements with the same valence state have different effects on the defect structure of the  $\text{Cu}_2\text{O}$  corrosion product and corrosion rate. For example,  $\text{Ni}^{2+}$  is more powerful than  $\text{Zn}^{2+}$ . However, it is known that a greater amount of nickel is retained in the corrosion product (1).

The shape of the weight loss versus time curve (parabolic decreasing) can be explained by two factors therefore. The first is a gradual thickening of the  $\text{Cu}_2\text{O}$  corrosion product. The second factor is incorporation of alloying elements into the corrosion product film. Any external factors which influence either the growth kinetics, defect



structure, or stability of this film will considerably influence corrosion performance.

The external factor, as discussed above, which appears to receive the majority of attention is polluted sea water containing sulfides. Among the principal sources of sulfides in sea water are action of sulfate reducing bacteria under anoxic (oxygen free) conditions on the natural sulfate content of the sea water, and putrefaction of organic sulfur compounds (proteins, etc.) from sanitary or industrial sewage (11). Oxygen free conditions may occur, especially in late summer, when organic matter largely uses up the dissolved oxygen. Partial putrefaction of organic sulfur compounds may result in the formation of organic sulfides such as cystine or glutathione. Cystine is present in many seaweeds and can be released by bacterial action; it is present in off-shore and in-shore waters but especially in large amounts in harbors and estuaries where organic material is being broken down. When hydrogen sulfide is present in the water, a non-protective black film containing copper sulfide can form on the surface of previously unexposed alloys (4).

This film is more noble (23,24) up to 50 millivolts (25), than the film normally formed in fresh sea water and behaves cathodically towards the underlying metal. Thus at a break in the sulfide film, corrosion would occur which could take the form of pitting, the sulfide film acting as the site of



the cathodic reaction. Bates and Popplewell (26) concluded that a corrosion product film of  $\text{Cu}_2\text{O}$  with even small amounts of  $\text{Cu}_2\text{S}$  appears to be highly defective and much less protective than one in which  $\text{Cu}_2\text{S}$  is absent.

It should also be recalled at this point, as discussed earlier, that sulfide environments where oxygen is absent does not cause greatly accelerated corrosion of the copper-base alloys. However, when oxygen is introduced in combination with sulfide, corrosion does occur at an accelerated rate and takes on a pitting form. This type of behavior is well documented in the literature.

A primary pollutant mentioned previously is ammonia. The effect of ammonia on the accelerated corrosion phenomenon has been relatively undocumented. However, laboratory tests showed that 10 ppm of  $\text{NH}_4^+$  were effective in causing pitting of aluminum brass but were not as effective as hydrogen sulfide (4). How this small amount of data relates to the effect of ammonia on copper-based alloys and the accelerated corrosion of same is relatively unknown. However, it is known that ammonia reacts with copper by the formation of a complex. The possibility exists that this same type of reaction may occur with copper-based alloys.

Perhaps the most widely used method of attempting to control the accelerated corrosion problem is by the use of ferrous sulfate as an inhibitor. Recent studies have shown



that practical corrosion control can be achieved by the introduction of ferrous sulfate into the sea water being carried by cupro-nickel piping systems, although the environmental impact of ferrous sulfate in waste water is an important consideration (27). Ferrous sulfate has frequently been utilized as an inhibitor to control aluminum-brass tube corrosion problems, and was simply extended to the use with cupro-nickel piping systems. The U. S. Navy has been carrying out experiments to explore methods to control accelerated corrosion of cupro-nickel alloys, and these experiments form the basis of the discussion to follow here.

The inhibiting effect of ferrous sulfate has been attributed to the generation of a film consisting primarily of lepidocrecite ( $\gamma$  -  $\text{FeO}\cdot\text{OH}$ ) which is electrophoretically deposited on cathodic areas of the copper alloy from the solution (29). This film reduces oxygen transport to the cathode thereby increasing the rate of cathodic polarization. It has been applied by methods ranging from monitored solution injection to daily batch additions of the crystals to inlet water, in a variety of concentrations generally around 1 ppm (28). The objective of the Navy study was to determine the effectiveness of ferrous sulfate as an inhibitor for sulfide-induced corrosion of cupro-nickel alloys as the result of short-term high-concentration sulfide exposure and long-term low-concentration sulfide exposure. Results obtained



indicated that only continuous treatment with ferrous sulfate was effective in suppressing corrosion caused by the high-concentration (0.2 ppm) sulfide transient (28). During injection, sulfide concentration was immediately reduced by more than an order of magnitude. However, continuous injection had an undesirable side effect in that a sludge of ferric hydroxide was deposited (28). The beneficial effects of continuous ferrous sulfate treatment is apparently due to both the ability to limit the available corrosion-accelerating sulfides as well as direct corrosion inhibition effects. None of the intermittent ferrous sulfate inhibitor application sequences investigated was totally effective in countering corrosion due to the high sulfide transient. Corrosion caused by long-term, low-concentration (0.01-0.04 ppm) sulfide pollution, on the other hand, was significantly reduced by intermittent inhibitor injection, with a period of 20-40 days being required to reach maximum effect (28). The treatment was more effective with alloy 715 than with alloy 706 (28).

In summary, it can be said that there are many theories about the accelerated corrosion phenomenon, but all of them remain unproven. An overall observation is that the corrosion resistance of cupro-nickel alloys depends critically upon the formation of a protective oxide film. The various pollutants in the sea water environment somehow cause the detriment of



the protective oxide film, thus decreasing the metal's corrosion resistance. As a result, the accelerated corrosion problem exists, and may increase in importance in harbors and fitting out basins where pollution levels tend to increase over time.



## CHAPTER 3

Materials and Test MethodsA. Experimental Methods

The preliminary objectives of this project were the construction of a recirculation loop suitable for a corrosion study and a reliable method of measurement of the velocity of the recirculating fluid within the loop. These objectives were satisfied by the use of polyvinyl chloride (PVC) pipe and a "short pipe orifice" pressure measurement technique. A discussion of specifics follows.

One of the primary considerations in the construction of a recirculation loop is the elimination of all metal that could possibly corrode or interfere with the metal sample of interest. The elimination of extraneous metal from the system was achieved by the use of standard PVC schedule 40 plastic pipe. In conjunction with this plastic pipe, a pump was chosen with all high grade plastic internals and a plastic reservoir container. The pump chosen was rated at 1/2 horsepower and approximately 40 gals/min maximum pumping capacity. The reservoir chosen was of a total capacity of 30 gallons. Arrangements for the insertion of the cupro-nickel samples were made by the use of high grade, hard rubber hose using standard 1-1/4" hose



clamps to achieve a water tight seal. All metal to plastic, metal to metal, or plastic to plastic connections were made in this fashion. Figure 4 shows a schematic of the recirculation loop.

The rationale for the loop arrangement used was as follows. By using a 1-1/2 inch discharge reduced to two 3/4" loops, two samples could be used concurrently. One recirculation loop led through a 36 inch length of metal pipe identical to the sample material, then through the sample material back to the reservoir. This 36 inch length of pipe allowed the flow to become fully developed (turbulent flow) (3), thereby reducing as much as possible the effects of piping bends. The other recirculation loop led through two 90° elbows and immediately into the metal pipe sample, thereby introducing as much turbulence as possible. It should be emphasized at this point that the fluid flow through the pipe is always turbulent. The Reynold's number was calculated to be approximately 25,000, with the transition from laminar to turbulent flow in pipes occurring in the range of 2300-4000. The distinction here is the term "fully developed" turbulent flow, as opposed to turbulent flow influenced by entrance effects. It is quite apparent that this recirculation loop arrangement is an attempt to evaluate the effects of sharp piping bends on the accelerated corrosion phenomenon. Both recirculation loops led



back to the reservoir after passing independent "short pipe orifices" which were used to monitor the fluid velocity within the pipe.

The "short pipe orifices" used in the recirculation loop were constructed by machining different diameters of PVC pipe to fit within one another and then joining them together. References 30 and 31 were used as guidance in the construction of the orifices. Two specific requirements that needed to be met (as dictated by References 30 and 31) were that the length of the "short pipe orifice" be  $(2.5 \text{ to } 3.0) \times \text{diameter}$ , and that the ratio of throat diameter to pipe diameter be between 25% and 70%. Both requirements were met. Figure 5 is a schematic of the "short pipe orifice" used. Both "short pipe orifices" were calibrated as a function of pressure drop using a positive displacement water meter to measure total volume flow in cubic feet per unit of time. Figure 6 is a plot of the data generated from this calibration procedure. The water meter was then removed from the system and the pressure drop used as a function of velocity during the experiments.

## B. Materials

Both alloy 706 and alloy 715 were available for use, but due to time constraints, and the fact that alloy 715



is considered more resistant to accelerated corrosion, it was chosen as the material to be used. The material was obtained at a Naval shipyard out of the standard Navy stock. It was Level I, alloy 715, 1.05 x .120, 25/32" I.D. No precleaning or pretreatment of any kind was done prior to insertion of the samples into the test loop in order to simulate actual service conditions of the piping. The samples used were 6 inches in length and machined at both ends to achieve a smooth 90° surface. After being run in the test loop, the samples were cut lengthwise to aid examination and analysis of the inner surface.

### C. Test Equipment

The test equipment used for this project was relatively standard. The pump chosen, as discussed earlier, was a 1/2 horsepower, 3450 rpm centrifugal pump by ITT MARLOW Model 2HU15ED-A3. A standard pH meter was used to determine the pH of the fluids of interest. It was a Beckmann Expandomatic SS-2. The potentiostat used to measure the potential of alloy 715 was a standard G. Bank Elektronik Wenking potentiostat. All potentials were measured against a standard calomel electrode. These four items were used throughout the project.



#### D. Test Procedures

The parameters chosen for experimentation purposes were very critical, especially the levels of pollution to be used. It must be kept in mind that if sulfides are added to the salt water, they will rapidly react with the oxygen in the water, thereby depleting the solution of corrosive sulfides by the formation of sulfur oxyanions, such as  $\text{SO}_3^-$ ,  $\text{SO}_4^-$ , and  $\text{S}_2\text{O}_3^-$  (3). In an attempt to combat this effect and ensure that a sufficient level of sulfides are available for reaction with the metal, it was decided to add sulfides to the water each working day. It is obvious that this will not maintain a constant level of sulfide pollution, but will alternate between a low sulfide/high sulfide condition, and will form the basis for a comparative analysis of different environments.

Seven different environments were tested, each with a basic salt solution of 3.4% NaCl buffered with 0.02%  $\text{NaHCO}_3$  (all percentages on a weight basis). The environments used were as follows:

- Sample 1 - 3.4% NaCl + 0.02%  $\text{NaHCO}_3$
- Sample 2 - 3.4% NaCl + 0.02%  $\text{NaHCO}_3$  + 10 ppm  $\text{NH}_4\text{Cl}$
- Sample 3 - 3.4% NaCl + 0.02%  $\text{NaHCO}_3$  + 10 ppm  $\text{NH}_4\text{Cl}$  + 10 ppm  $\text{Na}_2\text{S}$  (daily)
- Sample 4 - 3.4% NaCl + 0.02%  $\text{NaHCO}_3$  + 10 ppm  $\text{Na}_2\text{S}$  (daily)



Sample 5 - 3.4% NaCl + 0.02% NaHCO<sub>3</sub> + 10 ppm  
NH<sub>4</sub>Cl (daily)

Sample 6 - 3.4% NaCl + 0.02% NaHCO<sub>3</sub> + 10 ppm  
NH<sub>4</sub>Cl (daily) + 10 ppm Na<sub>2</sub>S (daily)

Sample 7 - 3.4% NaCl + 0.02% NaHCO<sub>3</sub> + 10 ppm  
NH<sub>4</sub>Cl (daily) + 10 ppm Na<sub>2</sub>S (daily)  
+ 1 ppm FeSO<sub>4</sub> (daily)

For each particular environment, two samples were exposed, as shown in Figure 4. One sample was exposed to fully developed turbulent flow (hereafter referred to as the outer loop), and the other sample to turbulent flow influenced by 90° piping bends (hereafter referred to as the inner loop). Each set of samples was exposed to the environment of interest for a period of 120 hours at a flow velocity of 5 ft/sec. The velocity of 5 ft/sec was chosen for two reasons. First and foremost, it was the minimum flow velocity achievable in the flow loop constructed (determined by the ability of the orifice meter to measure pressure). Second, this velocity was at or below the known breakaway velocity of alloy 715, as discussed earlier in Chapter 2. However, it should be realized that the breakaway velocity is a function of the pipe diameter (15). Decreasing the pipe diameter will decrease the thickness of both the velocity boundary layer and the diffusion boundary layer. A decrease in the velocity boundary layer thickness leads to an increased velocity gradient and hence an increased shear stress at the wall.



A decrease in the diffusion boundary layer thickness will often lead to an increased concentration gradient and hence an increased mass transport rate. Therefore, if surface film breakdown and metal removal are related to the surface shear stresses, or if the corrosion process is controlled by mass transfer to or from the surface, a decrease in the pipe diameter would be expected to result in an increased erosion-corrosion rate and a decreased breakaway velocity. The net result of this is that a velocity of 5 ft/sec will most likely be above the breakaway velocity of alloy 715 for 3/4" pipe.

The environments used have been detailed, but it should be mentioned why the particular compounds used were chosen.  $\text{Na}_2\text{S}$  was used as a source of sulfide since alkali sulfides are easily soluble in water and a solid of this type is relatively easy to work with.  $\text{Na}_2\text{S}$  was added to the water every 24 hours to achieve the desired level of at least 10 ppm's of sulfide, hereafter referred to as the "sulfide" environment.  $\text{NH}_4\text{Cl}$  was used as a source of ammonia since ammonium salts are completely ionized in water.  $\text{NH}_4\text{Cl}$  was added to the water at the beginning of the 5 day cycle to achieve a level of 10 ppm's of ammonium ion, hereafter referred to as the "low ammonia" environment.  $\text{NH}_4\text{Cl}$  was also used to add 10 ppm's of ammonium ion to the water daily, hereafter referred to as the "high ammonia" environ-



ment.  $\text{FeSO}_4$  was used as an inhibitor on sample number 7, simply because it is well known as an inhibitor.  $\text{FeSO}_4$  was added to the water to achieve a level of 1 ppm of iron ion. It should be remarked again that all numbers given as ppm are on a weight basis.

For each environment used, potential measurements of the clean metal in stagnant solution versus the standard calomel electrode were taken. Also, pH measurements of the solution of interest were taken. For comparative purposes and general interest, a small sample of alloy 715 was also allowed to corrode in a stagnant solution of the same composition as the 7 environments detailed earlier.

At this point, flow experimentation was essentially complete. The samples were cut lengthwise and readied for further examination.

#### E. Sample Examination

All samples were examined visually and with the aid of a stereo-microscope. Macroscopic metallography was used to aid in characterization of the surface. Microscopic metallography was accomplished by the use of the Scanning Electron Microscope, both for viewing the surface and for identification of surface constituents. For a more detailed and reliable characterization of surface constituents, use was made of Scanning Auger Microprobe Analysis. All of these methods were used in an attempt



to characterize the surface in both appearance and composition, and to attempt to analyze the mechanisms of accelerated corrosion, specifically as related to present theory and to the synergistic effect of ammonia.



## CHAPTER 4

Results and DiscussionA. Results

The experimental procedures outlined in Chapter 3 were carried out and the results are presented here. Water temperature throughout the experiments was  $44^{\circ}\text{C} \pm 1^{\circ}\text{C}$ . It should be noted that this water temperature coupled with the experimental velocity of 5 ft/sec placed these experiments on the border between Region A and Region B of Figure 2, the area of intermediate to maximum corrosion. One interesting visual effect perceived during experimentation was that when sulfide was added to the solution, the water immediately became dark brown and a sulfide odor was evident. Twenty-four hours later, just prior to the addition of more sulfide, the water appeared relatively clean and unpolluted with no evidence of sulfide odor. This curious effect was most likely due to the reaction of sulfides with oxygen to form stable ions and depleting the solution of sulfide ions.

PH and open circuit potential readings were taken for the first four solutions (salt, salt + low ammonia, salt + low ammonia + sulfide, salt + sulfide) to see if significant changes were occurring. It should be noted



that the normal pH of sea water is 8.1 - 8.3. PH readings were taken both before and after the addition of sulfides to determine if significant changes were occurring. Electrode potential versus the standard calomel electrode was also measured in the first four solutions both before and after the addition of sulfides, allowing 24 hours for the readings to stabilize. The results are presented in tabular form in Figure 7. As can be seen from Figure 7, pH in solutions without sulfides remained constant at 8.3, while solutions with sulfides were 8.3-8.4 prior to the addition of more sulfides and 8.7-8.8 after. Electrode potential in solutions without sulfides was constant at -210mv, while sulfide-containing solutions maintained a less noble potential of -130mv, regardless if the readings were taken before or after the addition of sulfide.

All seven samples were examined visually, both under low and high magnification. A brief description of each sample follows, and it should be remembered that the following shorthand terminology was used:

Inner loop - turbulent flow influenced by 90° bends

Outer loop - fully developed turbulent flow

Salt - 3.4% NaCl + 0.02% NaHCO<sub>3</sub>

Low Ammonia - 10 ppm NH<sub>4</sub><sup>+</sup> using NH<sub>4</sub>Cl

Sulfides - 10 ppm S<sup>-2</sup> per day using Na<sub>2</sub>S



High Ammonia - 10 ppm  $\text{NH}_4^+$  per day using  $\text{NH}_4\text{Cl}$

Ferrous Sulfate - 1 ppm  $\text{Fe}^{++}$  per day using  $\text{FeSO}_4$

Sample 1: (Salt)

As can be seen from Figure 8, there appears to be a thin oxide film on the surface, although it does not bear the reddish color expected of  $\text{Cu}_2\text{O}$ . There is no evidence of pitting or other abnormal corrosion. No difference in appearance existed between the inner and outer loops. The sample immersed in stagnant solution appeared to have a grayish oxide film partially covering the surface, but thicker than the film formed in the flowing solution. Again, there was absolutely no evidence of accelerated corrosion.

Sample 2: (Salt + Low Ammonia)

This sample was the first test of ammonia acting alone as a contaminant. The results were completely negative. Figure 9 shows the sample in question, and as can readily be seen, it is essentially identical in appearance to Figure 8 (Sample 1). Again, there is no evidence of pitting, nor any difference between the inner and outer loops. The sample immersed in stagnant solution was identical in appearance to sample 1. There was no evidence of accelerated corrosion.

Sample 3: (Salt + Low Ammonia + Sulfide)

The appearance of this sample was altered substantially from the first two by the addition of sulfides to the



solution. The entire surface was covered by a thin, dark brown film, with very general finely-sized pitting dispersed over the surface. As can be seen from Figure 10, the dark film was wiped away on half of the sample to allow comparison of the two halves. It should be noted that the film was thin enough to allow pitting to be seen through it. When the sample was viewed with the dark film intact, it could be seen that the pits had a greenish white corrosion product covering them. When the dark film was wiped away, the majority of the corrosion product was also removed revealing the bright silver base metal interior to the pits surrounded by a reddish film. There was no significant difference between the inner and outer loops. The sample immersed in stagnant solution had a thick film brownish in color, but still no indication of pitting or other abnormal corrosion.

Sample 4: (Salt + Sulfide)

The sample was the first and only sample tested with sulfide as the only contaminant. It exhibited the same thin, dark brown film as found on sample 3, but the corrosion pits were noticeably fewer in number and slightly larger in size, as can be seen from Figure 11. The corrosion pits have still retained the greenish white corrosion product present on sample 3. Also unchanged was the reddish layer laying beneath the dark brown film and surrounding the



corrosion pits. Again, there was little difference between the inner and outer loops, and the sample in the stagnant solution was substantially identical to sample 3. In effect, samples 3 and 4 were identical except for the number and size of the corrosion pits.

Sample 5: (Salt + High Ammonia)

This was the first attempt to generate pitting corrosion by increasing the amount of ammonia in the solution. The results were negative, in that there was essentially no difference between this sample and samples 1 and 2 discussed earlier. See Figure 12.

Sample 6: (Salt + High Ammonia + Sulfide)

Whereas the increase in ammonia when it was the only contaminant had little effect, the same procedure in the presence of sulfide exhibited several noticeable effects. Firstly, the dark brown film, which was thin and smooth earlier, became very thick and flaky. Figure 13 shows the film and its very thick, flaky nature. When the nonadherent film was removed, there was a metallic surface underneath it, similar to the interior of a corrosion pit. Figure 14 shows the same sample with part of the flaky film removed, revealing the extensive corrosion beneath. The areas that were still intact were reddish in color, indicating the presence of the same film discussed in previous samples. Figure 15 shows the effect of the increase in ammonia in the presence of



sulfide. It should be compared to Figure 10, which was the "Low Ammonia" sample. Again, there was little difference between the inner and outer loops. However, the stagnant solution sample had a darker and thicker brownish film than samples 3 or 4, although there was still no indication of pitting or film flaking.

Sample 7: (Salt + High Ammonia + Sulfide + Ferrous Sulfate)

This sample was an attempt to evaluate the effect of ferrous sulfate in reducing corrosion for the worst case, specifically sample 6. To ensure that more sulfides were only added to the water in the presence of the inhibitor, ferrous sulfate, ammonium chloride, and sodium sulfide were added to the solution in that order. The use of the inhibitor had a noticeable positive effect on the extent of corrosion observed, as can be seen from Figure 16. The thick, dark brown, flaky film observed on sample 6 became thinner (similar to samples 3 and 4), and took on a greenish hue. The change in color was no doubt in response to the addition of ferrous sulfate to the solution. The dark film was still flaky, but much less so than sample 6. Underneath the dark covering film was still the reddish layer, although it too had taken on a greenish hue. The sample immersed in stagnant solution took on a film with a greenish hue with areas of dark brown, similar to sample 6. There was still no indication of any pitting corrosion or flaking of the surface film. Also,



both inner and outer loops were again nearly identical in appearance.

The general results listed for each sample were based simply on a visual examination. Several items should be emphasized. First, at the velocity of fluid used (5 ft/sec), there was essentially no difference between the inner and outer loops for all the samples tested. Second, the samples immersed in stagnant solution had a thick corrosion film on them, but no evidence of pitting or other abnormal corrosion. Third, potential and pH readings were relatively stable for the two situations discussed (with or without sulfides).

The next logical step in the analysis of the samples would be the identification of the surface films discussed earlier. Toward this end, both the Scanning Electron Microscope (SEM) and Scanning Auger Microprobe Analysis (SAM) were used in an attempt to determine surface constituents.

The SEM was used to analyze two samples which contained the surface films of interest, specifically the following: (1) thin, dark film, (2) thick, flaky film, (3) pit corrosion product, (4) reddish film, and (5) base metal inside a pit. Sample 4 (Salt + Sulfide) and sample 6 (Salt + High Ammonia + Sulfide) were used as representative samples. Sample 4, it will be remembered, contained widely spaced pits slightly larger than sample 3 (Figures 10 and 11). Figure 17 shows a representative pit from sample 4 with the



thin, dark film removed but partial corrosion product still intact. Figure 18 shows the transition from the cleaned area to the area covered by the thin, dark brown film complete with a corrosion product covered pit. It should be noticed that the dark film is loose but not at all of a flake nature. Figure 19 is a high magnification of the thin, dark brown film showing its loose, powder-like characteristics. An Energy Dispersive X-Ray Analysis (EDAX) scan of the thin, dark film is reproduced in Figure 20, showing the sulfur to be a primary constituent, and otherwise dominated by copper. Primarily for completeness, Figures 21 and 22 are included showing respectively: (1) a corrosion pit with corrosion product partially intact, and (2) a high magnification of a three-way junction of the inner pit base metal, the corrosion product, and the corrosion film. Sample 6 (Figures 14 and 15) did not reveal any significant differences from sample 4, other than the thickness of the dark corrosion film discussed earlier. Figure 23 is a slightly higher magnification than before showing the flakiness of the film and its nonadherence. The actual identification of the surface films, to the extent of the capability of EDAX, was as follows:

- (1) The pit corrosion product was high in copper and high in chloride.
- (2) The reddish corrosion film was high in copper and high in nickel, with copper dominating.



EDAX could not identify oxygen as a constituent.

- (3) The dark brown film was high in copper, high in nickel, and high in sulfur. This was true regardless if ammonia was present or not.
- (4) The base metal in a pit was high in nickel but low in copper, compared to the unpitted base metal which was high in both copper and nickel with copper dominating.

It should be emphasized that the above results held true for both sample 4 and sample 6.

In an attempt to verify the results from EDAX and to possibly identify oxide films on the surface of the samples, a Scanning Auger Microprobe (SAM) was used. The same two samples were used as before, but adverse effects due to the sample charging hindered the analysis. The basic results of SAM analysis were essentially the same as those from EDAX. Perhaps the best output from SAM was a spot scan in an area of the dark brown film indicating high levels of copper and sulfur as was expected from the EDAX results. One major problem with SAM for use on these specific samples was its extreme sensitivity to contaminants on the surface. Since these samples could not be cleaned for fear of removal of corrosion products or non-adherent films, an exact identifi-



cation of surface films could not be made, specifically the identification of  $\text{CuCl}$  and  $\text{Cu}_2\text{O}$ . One very interesting aspect of the SAM analysis was the line scans performed. Figure 25 is a line scan of sulfur passing from the dark film area to the lighter reddish area, with points above and below the line signifying the presence or absence, respectively, of sulfur. Figures 25 and 26 were line scans of a corrosion pit, with the corrosion product removed, showing the relative presence of copper and nickel. This was the same result given by EDAX analysis. No other specific conclusions could be reached as a result of SAM analysis.

## B. Discussion

The analysis of corrosion product films was not really conclusive in the area of oxides. The experimental observations discussed in chapter 2 identified the oxide film as  $\text{Cu}_2\text{O}$  which is reddish in color (32) and appears to be the reddish film discussed earlier. Reference to Figure 27, which is a Pourbaix diagram for pure copper, indicates that at the stagnant solution potential of  $-210\text{mv}$  (SCE) and a pH above 8.0, the corrosion film should indeed be  $\text{Cu}_2\text{O}$ , as expected. At the same pH but a potential of  $-130\text{mv}$  (SCE), however, the corrosion film should be  $\text{CuO}$ . Figure 28 is an experimental Pourbaix diagram for alloy 715 (34) and at the same pH and potentials as above, the alloy is again in the same region. These observations and the results discussed



earlier raise several questions. Why is  $\text{CuO}$  the likely corrosion product (at  $-130\text{mv}$ ) using Pourbaix diagrams, yet  $\text{Cu}_2\text{O}$  has been experimentally identified as the oxide film? Also, why do the stagnant samples show no pitting, yet the samples exposed to flowing solutions do, both being exposed for the same period of time? These differences are more than likely explained by the fact that potentials observed under conditions of flowing liquid may be substantially different from those observed under stagnant conditions, as will the shear forces acting on the films. At any rate, it will be accepted here that the oxide film is indeed  $\text{Cu}_2\text{O}$  in all cases, since it has been previously identified as such, and a visual examination indicates agreement. The next obvious film of concern was the brownish film discussed so often and identified as being high in copper and high in sulfur. Past experimental observations have identified this film as  $\text{Cu}_2\text{S}$ , and my observations indicate the same. Suffice it to say that  $\text{Cu}_2\text{O}$  was expected and found to be the dark brown film, regardless of the amount of ammonia present. The last corrosion film of consequence was the greenish white product covering the corrosion pits. The corrosion product was found to be high in copper and high in chloride, leading to its identification as cuprous-chloride (white) with another compound of copper (green) mixed in. This is a typical corrosion product for copper in sea water (pitting), and it



is not of major interest here. Perhaps the most interesting result of the analysis was that the pits (after removal of the corrosion product) were found to be high in nickel and low in copper. Although at first glance this seemed odd, it was not hard to visualize why it happened. The metal was originally 70% Cu and 30% Ni. Assume a pit formed in the surface and began to corrode, forming  $\text{CuCl}$ , thus depleting the local area (pit) of copper ions. When the corrosion product was removed, the copper atoms in it were removed also, leaving behind the base metal temporarily depleted in copper. How long this condition persists is a matter of conjecture, as is its importance to the present problem. In summary, from the results obtained in these experiments, it seems logical to accept the identification of surface films discussed in chapter 2 and repeated here. However, the role of ammonia must still be addressed, and will be treated later in this chapter.

The effects of several variables used during experimentation need to be discussed, specifically the effect of velocity and the inner and outer loops. As stated earlier, a fluid velocity of 5 ft/sec was chosen because it was at or below the stated breakaway velocity for alloy 715, and in this way the erosion effects hopefully would be minimized, since it is well established that the extent of accelerated corrosion increases with velocity. While

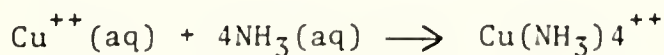


holding the velocity constant, an attempt was made to evaluate the effects of sharp piping bends on the corrosion phenomenon. As was stated earlier, these results proved negative (inner and outer loops), probably because of the low fluid velocity used. Again, it is well established that the adverse effects of sharp piping bends become more pronounced as velocity is increased. One other variable which should be mentioned is the tests done using stagnant solutions. As was stated earlier, no pitting or other abnormal corrosion, including non-adherence of surface films, was observed on any of the samples placed in stagnant solution. This merely verifies that accelerated corrosion is indeed an erosion-corrosion process.

Perhaps the most interesting part of this project was the effect of ammonia on the accelerated corrosion process. As was demonstrated earlier in this chapter, ammonia by itself did little damage in the short time of testing, even at high concentrations. Yet when ammonia was used in conjunction with sulfides, the extent of corrosion was considerably altered. This synergistic effect of ammonia and sulfide on cupro-nickel alloys has been relatively ignored in the literature, yet ammonia in varying concentrations is present in most inland harbors and waterways. I do not propose to offer a solution here, but I will propose a possible mechanism for the synergistic effect. It should



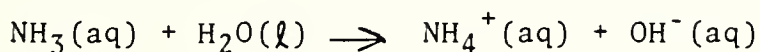
be remembered that the resistance of cupro-nickel alloys to accelerated corrosion is a strong function of the protective  $\text{Cu}_2\text{O}$  film that is formed on the surface. In fact, it will be recalled from chapter 1 that cupro-nickel piping exposed to clean sea water for a sufficient length of time was not affected by sulfide pollution. Any variable that alters this oxide film, especially during its early life, will increase the metal's susceptibility to corrosion. In the early life of the oxide film, sulfide contaminants combine with the copper in the metal to form  $\text{Cu}_2\text{S}$ , vice  $\text{Cu}_2\text{O}$  (Figure 29-A). The shear forces from the moving fluid strip the non-adherent  $\text{Cu}_2\text{S}$  from the surface forming the classical small anode-large cathode situation, hence pitting (Figure 29-B). When ammonia is present, the extent of corrosion increases perceptibly. The mechanism involved is a subject that has not been thoroughly addressed in the literature. It is well known that ammonia reacts with pure copper by formation of a complex such as (35):



It is reasonable to assume that a similar reaction occurs between ammonia and copper alloys. However, the accelerated corrosion phenomenon is dependent on the extent of  $\text{Cu}_2\text{O}$  formation, with copper being in the +1 valence state. In the sea water environment,  $\text{NH}_3$  is available for reaction



with  $\text{Cu}_2\text{O}$  to form a complex, but this reaction is doubtful since  $\text{Cu}_2\text{O}$  is a stable compound and  $\text{Cu}^+$  is easily oxidized and is stable only in very insoluble compounds such as  $\text{Cu}_2\text{O}$ , or complex ions such as  $\text{CuCl}_2^-$ . Therefore, it appears that a complexing mechanism is not the likely candidate as a cause for the increased corrosion observed. The other form of ammonia present in sea water and in the environments used in these experiments is the ammonium ion,  $\text{NH}_4^+$ . This ion can be produced by the reaction of  $\text{NH}_3$  with water (35):



Another likely source of  $\text{NH}_4^+$  ions would be from pollution sources such as ammonium salts. Whatever the source, when the ion  $\text{NH}_4^+$  is present, it is relatively stable and does not form complexes (35). From reference 33, it is seen that  $\text{Cu}_2\text{O}$  is soluble both in  $\text{NH}_4\text{Cl}$  and  $\text{NH}_4\text{OH}$ . The sea water environment can contain both of these, whether from the reaction of  $\text{NH}_3$  and  $\text{H}_2\text{O}$  mentioned previously, or from  $\text{NH}_4^+$  ions present from pollution and  $\text{Cl}^-$  ions naturally present in sea water. These two solvents, although present in very low concentrations, could still conceivably be strong enough to locally cause weakening or dissolution of the  $\text{Cu}_2\text{O}$  film, thus allowing the formation of  $\text{Cu}_2\text{S}$  which would subsequently be removed by velocity shear creating additional sites for pitting initiation (Figures 29-C and 29-D). The overall



result would naturally be that not only the original  $\text{Cu}_2\text{S}$  sites are available for pitting, but also the sites where  $\text{Cu}_2\text{S}$  has formed due to the weakening or dissolution of the  $\text{Cu}_2\text{O}$  film. The net result would be an increase in the number of corrosion sites, precisely what was observed (compare Figures 10 and 11). In this way, it is possible for ammonia to dramatically effect the extent of corrosion, yet in no way become incorporated into the corrosion films observed. This was seen for all samples with ammonia, and the explanation above is only a first order attempt to formulate a mechanism for the synergistic effect of ammonia in conjunction with sulfide.

### C. Conclusion

It is obvious that ammonia has a substantial effect on the resistance of cupro-nickel alloys to accelerated corrosion. One possible explanation was presented in this chapter. However, other mechanisms are possible, and the overall conclusion from this project must be that ammonia cannot be ignored when investigating the effects of sulfide contaminated sea water. Although sulfide-induced accelerated corrosion of cupro-nickel alloys has been well documented, and is at present still being investigated, the trend has been to concentrate on sulfide as a pollutant and not on the synergistic effect of ammonia and sulfide together.



Future research should focus more on this synergistic effect in order to further our knowledge of the phenomenon of accelerated corrosion when dealing with cupro-nickel alloys.



REFERENCES

1. James M. Popplewell, "Marine Corrosion of Copper Alloys: An Overview", National Association of Corrosion Engineers (NACE), Corrosion 78, Paper Number 21, March, 1978.
2. Corrosion Resistance of Copper and Copper Alloys, The American Brass Company, Waterbury, Connecticut, 1956.
3. D. D. Macdonald, B. C. Syrett, S. S. Wing, A Study to Determine the Mechanisms of Corrosion of Copper-Nickel Alloys in Sulfide-Polluted Seawater, SRI International Project No. PYU 6077, Annual Report, February, 1978.
4. D. C. Vreeland, CDR. E. G. Ogden, "Seawater Corrosion of 90/10 Copper-Nickel Piping - A Survey", Naval Ship Research and Development Center, Annapolis, Maryland, Report TM28-74-307, December, 1974.
5. E. M. Stanley, W. B. Mercer, A. M. Miller, "Characterization of the River Environment", Naval Ship Research and Development Center, Annapolis, Maryland, Report TM28-74-334, December, 1974.



6. D. C. Vreeland, "Review of Corrosion Experience with Copper-Nickel Alloys in Sea Water Piping Systems", Materials Performance, October, 1976.
7. T. W. Montemarano, F. A. Plummer, "Relationship of Materials and Fabrication Procedures to Accelerated Corrosion Behavior of 90/10 Copper-Nickel Shipboard Piping Systems", Naval Ship Research and Development Center, Annapolis, Maryland, Report TM28-75-24, April, 1975.
8. H. P. Hack, "Investigation of Accelerated Corrosion of Shipboard Piping", Naval Ship Research and Development Center, Annapolis, Maryland, Report TM28-77-180, June, 1977.
9. Accelerated Corrosion of Copper Nickel Piping, National Materials Advisory Board, Publication NMAB-343, National Academy of Sciences, Washington, D. C., 1977.
10. A. Cohen, P. F. George, Materials Performance, Vol. 13, No. 8, P. 26, 1974.
11. J. F. Bates, J. M. Popplewell, "Corrosion of Condenser Tube Alloys in Sulfide Contaminated Brine", Corrosion, August, 1975.



12. R. S. Bem, H. S. Campbell, Proceedings of the 1st International Conference on Metallic Corrosion, Butterworths, London, 1962.
13. B. C. Syrett, "Accelerated Corrosion of Copper in Flowing Pure Water Contaminated with Oxygen and Sulfide", Corrosion, July, 1977.
14. K. D. Efird, Corrosion, Vol. 33, No. 1, P. 3, 1977.
15. B. C. Syrett, "Erosion-Corrosion of Copper-Nickel Alloys in Sea Water and other Aqueous Environments - A Literature Review", Corrosion, June, 1976.
16. G. J. Danek, Naval Engineers Journal, Vol. 78, P. 763, 1966.
17. D. B. Anderson, "Factors Affecting Corrosion of Copper and Copper Alloys in Hot Sea Water", Paper presented at the Annual Meeting of the National Association of Corrosion Engineers, Chicago, Illinois, 1971.
18. R. F. North, M. J. Pryor, Corrosion Science, Vol. 10, P. 297, 1970.
19. J. M. Popplewell, R. J. Hart, J. A. Ford, Corrosion Science, Vol. 13, P. 295, 1973.

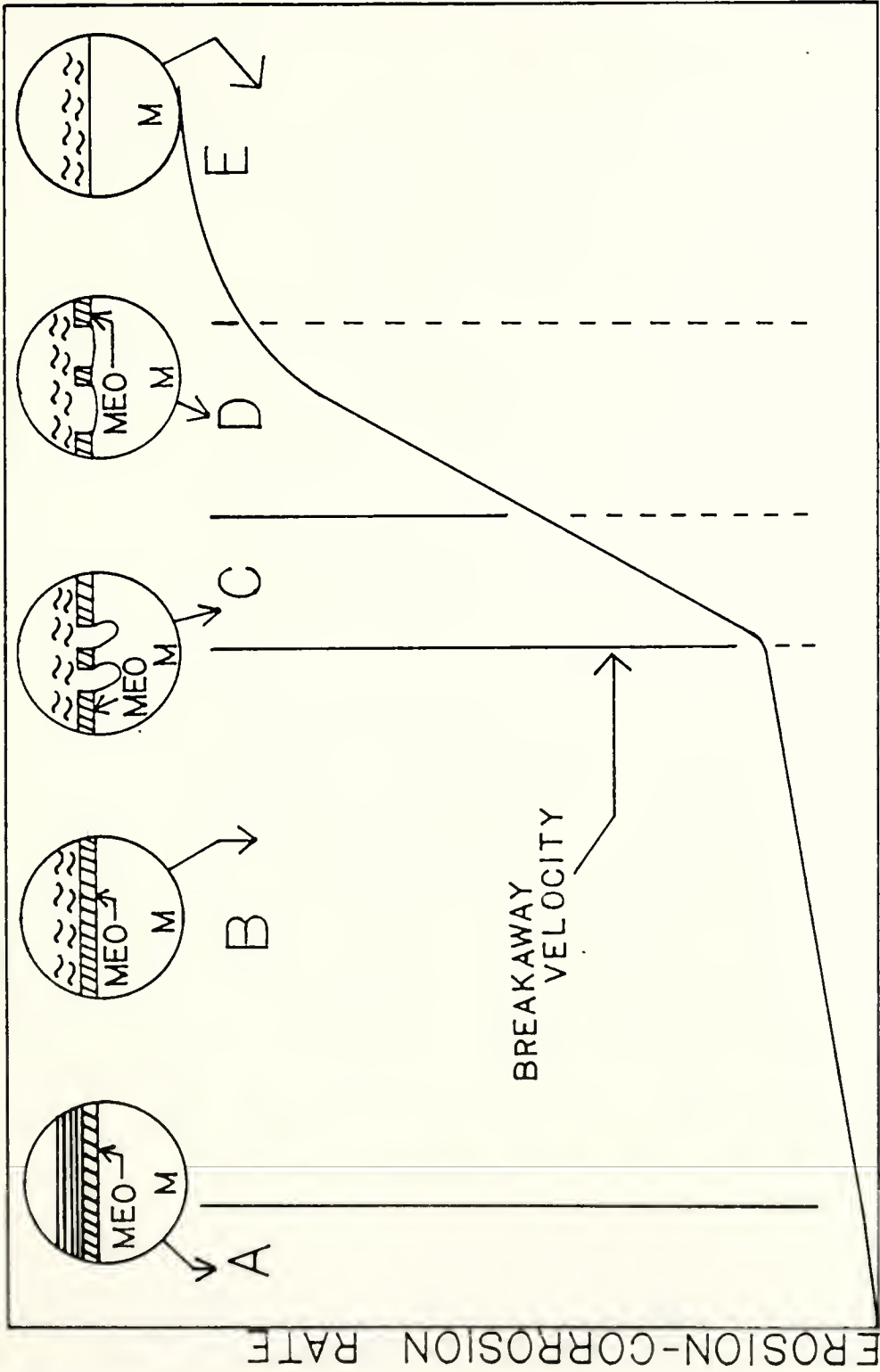


20. J. F. Bates, J. M. Popplewell, Corrosion, Vol. 31, No. 8, P. 269, 1975.
21. E. D. Mor, A. M. Beccaria, Corrosion, Vol. 30, No. 10, P. 354, 1974.
22. E. D. Mor, A. M. Beccaria, Br. Corrosion Journal, Vol. 10 (1), P. 33, 1975.
23. P. T. Gilbert, "The Resistance to Failure of Condenser and Heat Exchanger Tubes in Marine Service", Trans. Inst. of Marine Eng., Vol. 66, P. 1, 1954.
24. P. T. Gilbert, "Some Factors Affecting the Performance of Condenser and Heat Exchanger Tubes", Chemistry and Industry, July, 1959.
25. L. Kenworthy, "Some Corrosion Problems in Naval Marine Engineering", Trans. Inst. of Marine Eng., Vol. 77, P. 149, 1965.
26. J. F. Bates, J. M. Popplewell, "Corrosion of Condenser Tube Alloys in Sulfide Contaminated Brine", Paper #100, NACE Corrosion/74, Chicago, March, 1974.
27. F. A. Godshall, "The Environmental Impact of Ferrous Sulfate from Waste Water Discharge from Naval Vessel Heat Exchangers", Naval Ship Research and Development Center, Annapolis, Maryland, Report TM28-77-354, December, 1977.



28. H. P. Hack, J. P. Gudas, "Inhibition of Sulfide-Induced Corrosion of Copper-Nickel Alloys with Ferrous Sulfate", Paper No. 23, NACE Corrosion/78, Houston, March, 1978.
29. R. F. North, M. J. Pryor, "The Protection of Copper by Ferrous Sulfate Additions", Corrosion Science, Vol. 8, P. 149, 1968.
30. L. S. Marks, ed., T. B. Baumeister, ed., Mechanical Engineer's Handbook, McGraw-Hill Book Company, New York, 1958.
31. "Flow Measurement", ASME Power Test Codes, Part 5.
32. M. Pourbaix, Lectures on Electrochemical Corrosion, Plenum Press, New York-London, P. 264, 1973.
33. R. C. Weast, ed., Handbook of Chemistry and Physics, The Chemical Rubber Co., Cleveland, Ohio, 1970.
34. J. M. Bowers, "Crevice Corrosion of a 70/30 Chromium Modified Cupronickel and its Relationship to the Experimental Pourbaix Diagram", Thesis, M. S., University of Florida, 1973.
35. J. A. Campbell, Chemical Systems, W. H. Freeman and Company, San Francisco, 1970.





VELOCITY

EROSION-CORROSION RATE

BREAKAWAY VELOCITY

FIG. 1



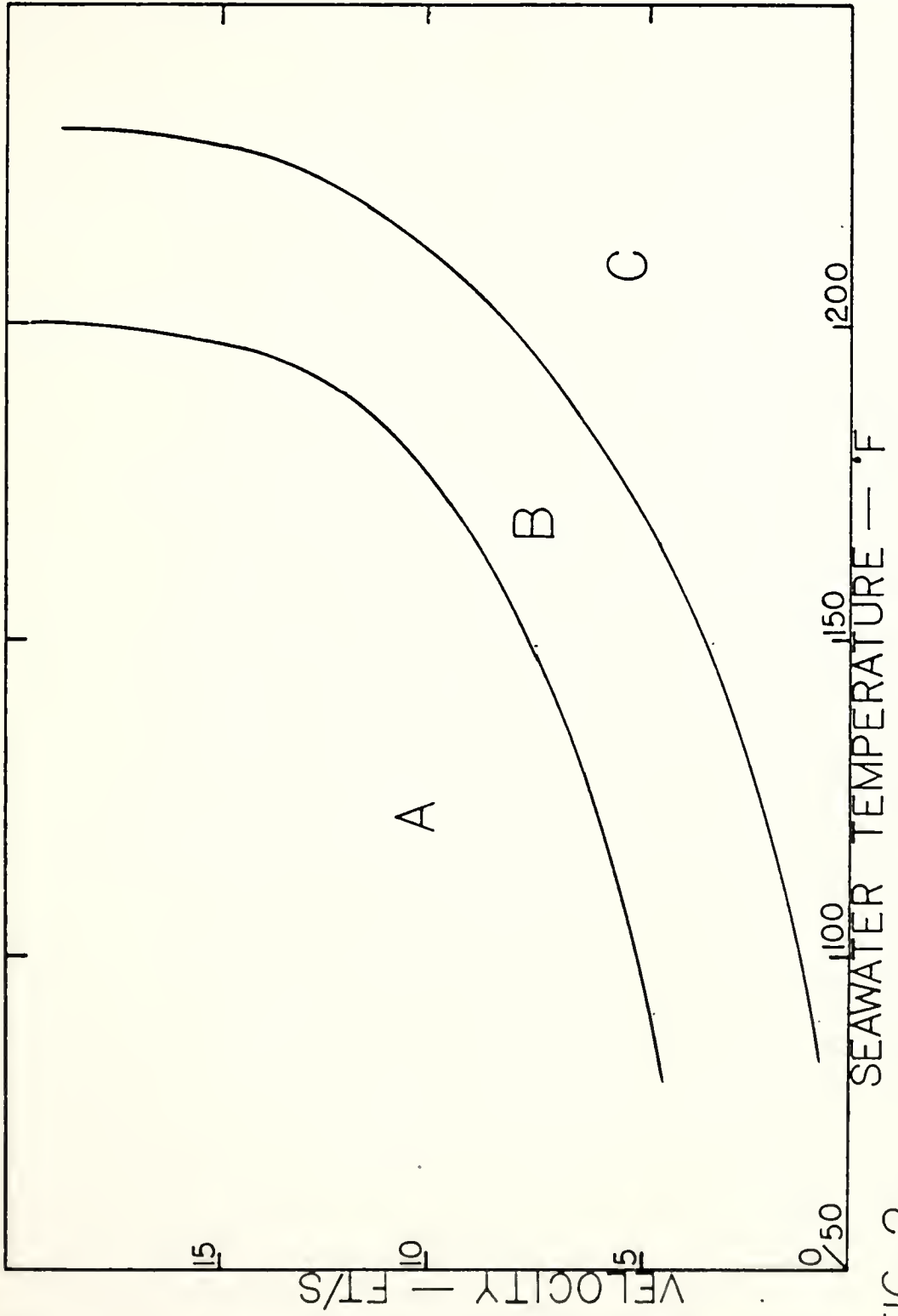


FIG. 2



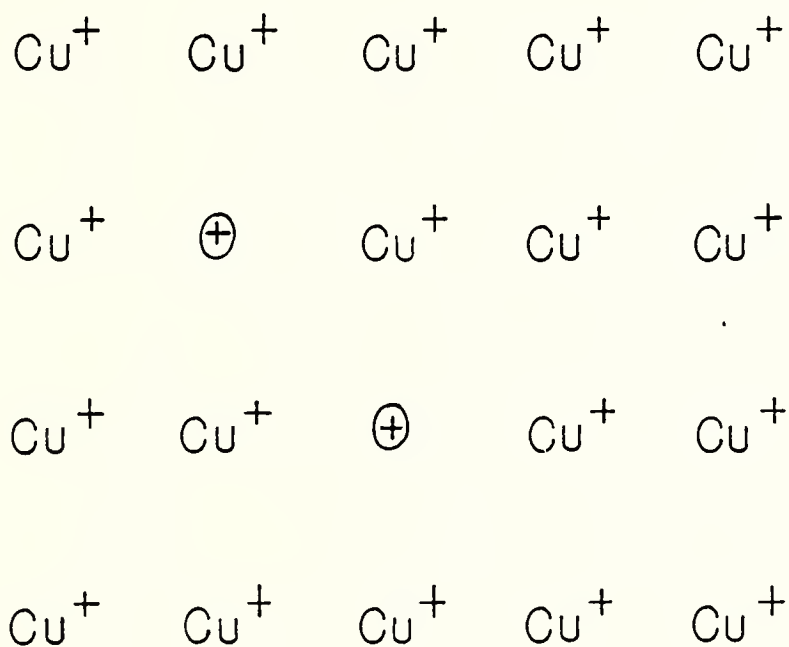
DEFECTIVE CATION LATTICE OF  $\text{Cu}_2\text{O}$ 

FIG. 3



RECIRCULATION LOOP

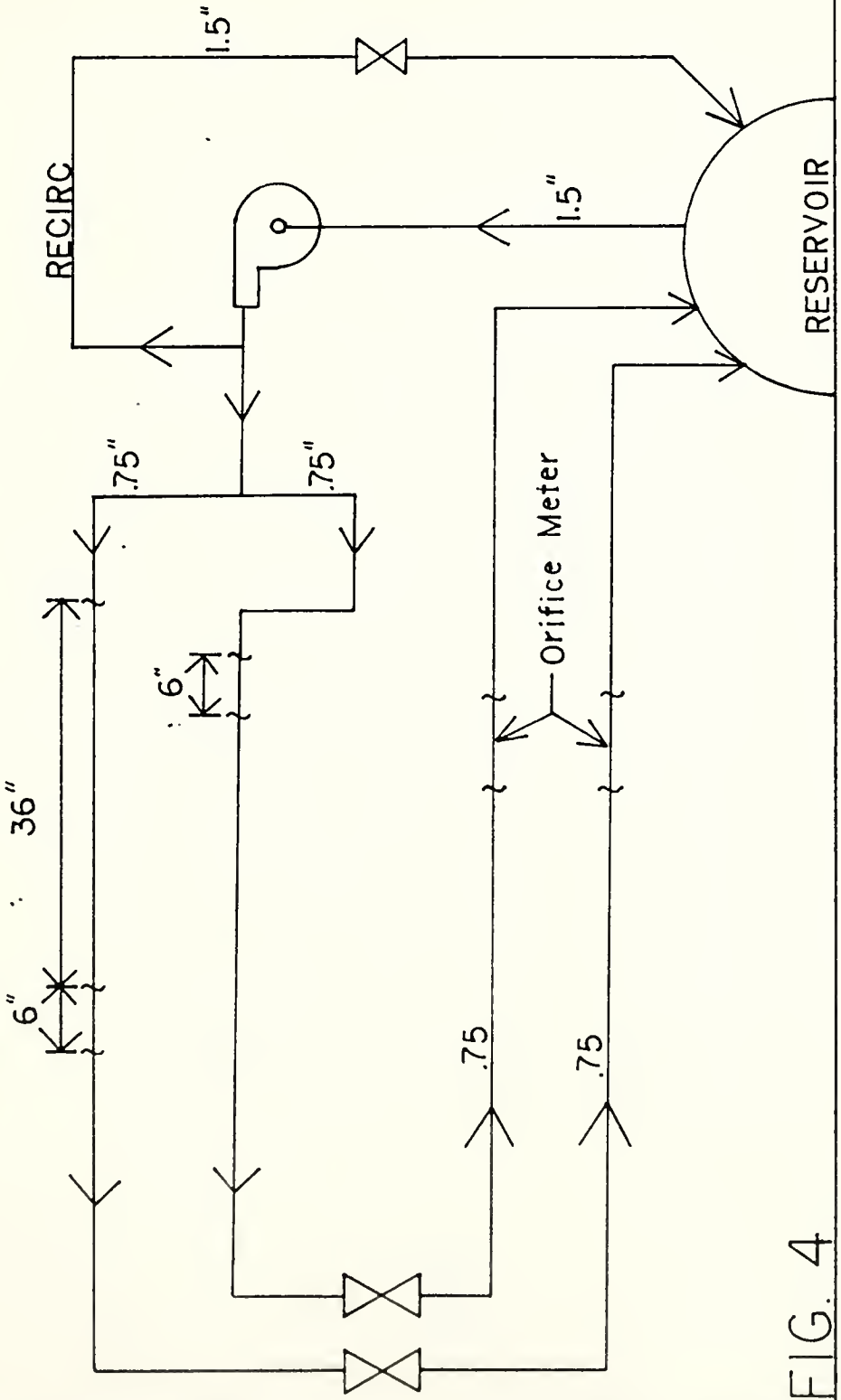


FIG. 4



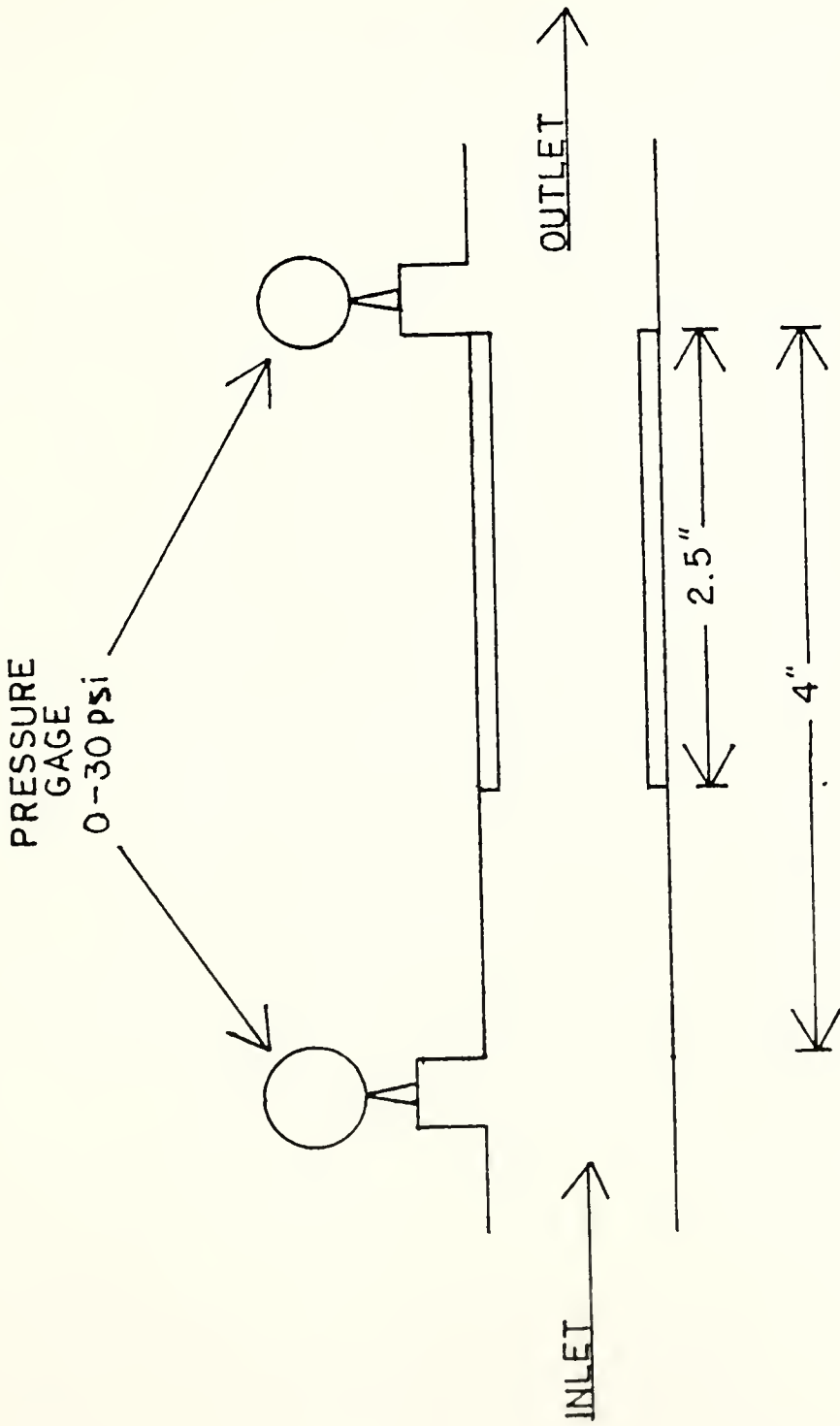


FIG. 5



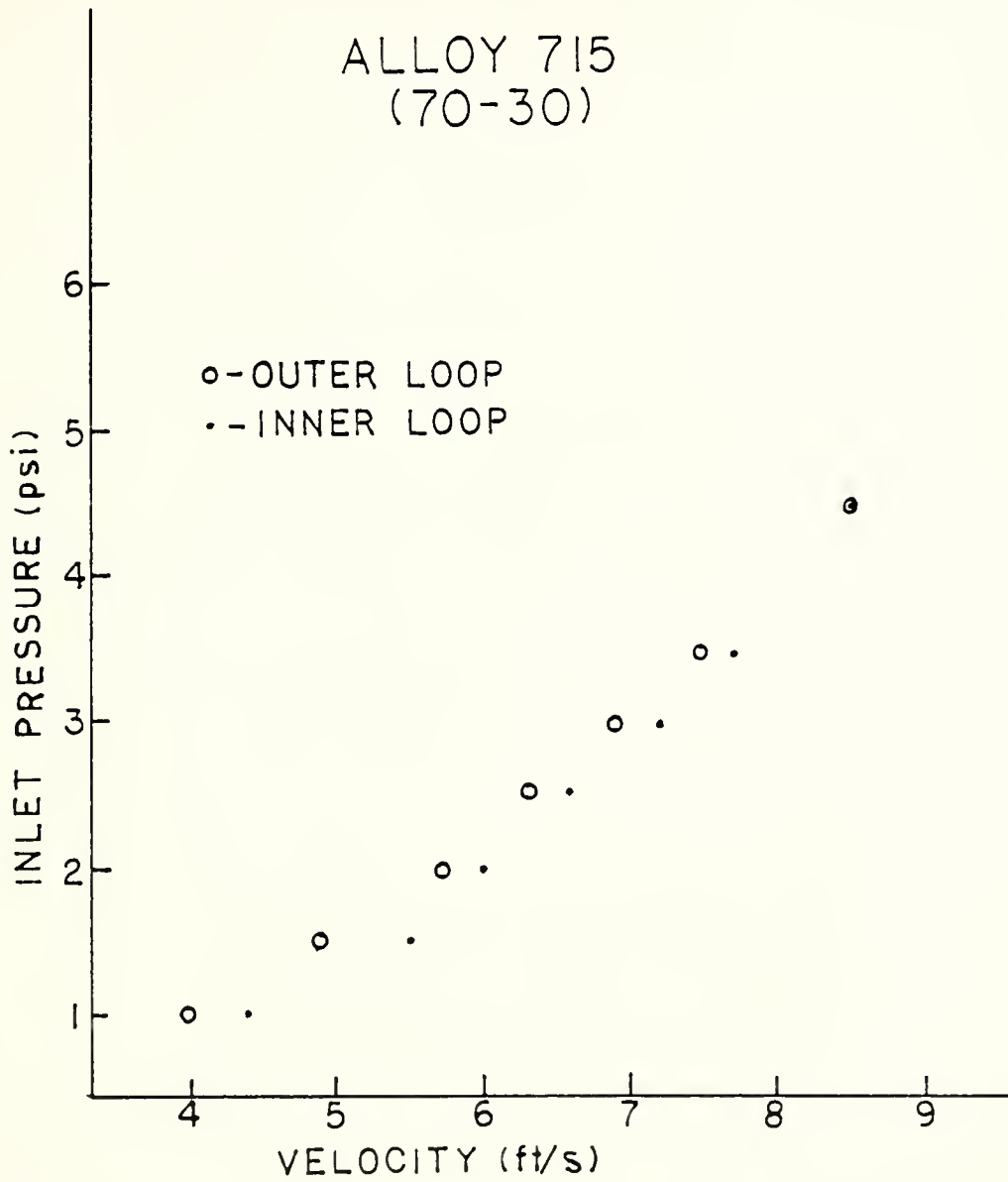


FIG. 6



|                              | PH     |       | POTENTIAL (mv) |       |
|------------------------------|--------|-------|----------------|-------|
|                              | BEFORE | AFTER | BEFORE         | AFTER |
| SALT                         | 8.3    | 8.3   | 210            | —     |
| SALT + LOW AMMONIA           | 8.3    | 8.3   | 210            | —     |
| SALT + LOW AMMONIA + SULFIDE | 8.3    | 8.7   | 130            | 130   |
| SALT + SULFIDE               | 8.4    | 8.8   | 130            | 130   |

EXPERIMENTAL VALUES

FIG. 7



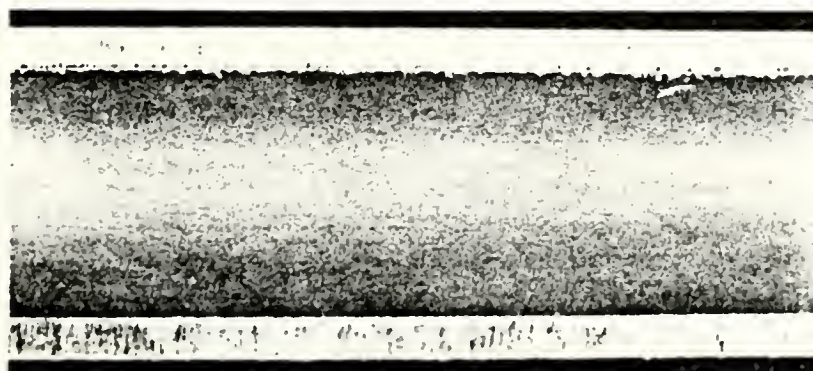
SALT



FLOW  
←

FIG. 8

SALT  
LOW NH<sub>3</sub>



FLOW  
←

FIG. 9

SALT  
LOW NH<sub>3</sub>  
SULFIDE



FLOW  
←

FIG. 10



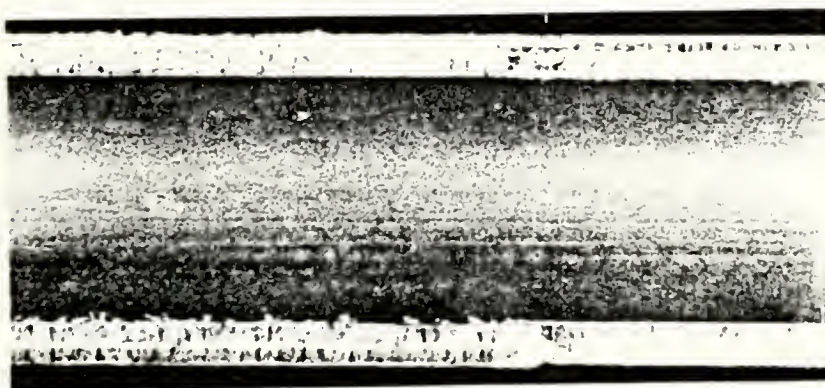
SALT  
SULFIDE



FLOW  
←

FIG. 11

SALT  
HIGH NH<sub>3</sub>



FLOW  
←

FIG. 12

SALT  
HIGH NH<sub>3</sub>  
SULFIDE



FLOW  
←

FIG. 13

40 X



SALT  
HIGH NH<sub>3</sub>  
SULFIDE

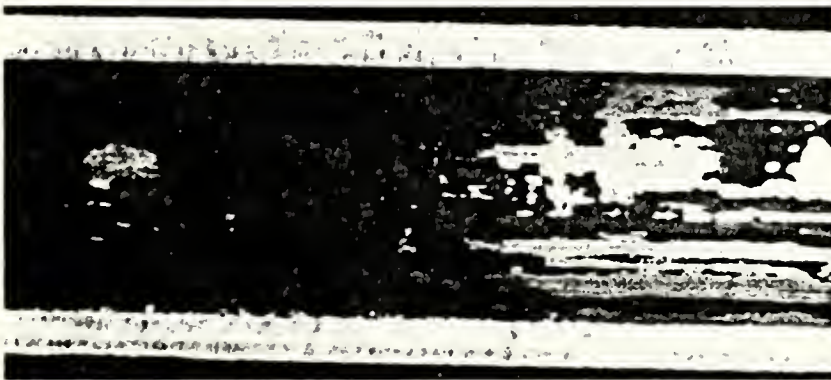


FLOW  
←

FIG. 14

40 X

SALT  
HIGH NH<sub>3</sub>  
SULFIDE



FLOW  
←

FIG. 15

SALT  
HIGH NH<sub>3</sub>  
SULFIDE  
FeSO<sub>4</sub>



FLOW  
←

FIG. 16



SALT  
SULFIDE

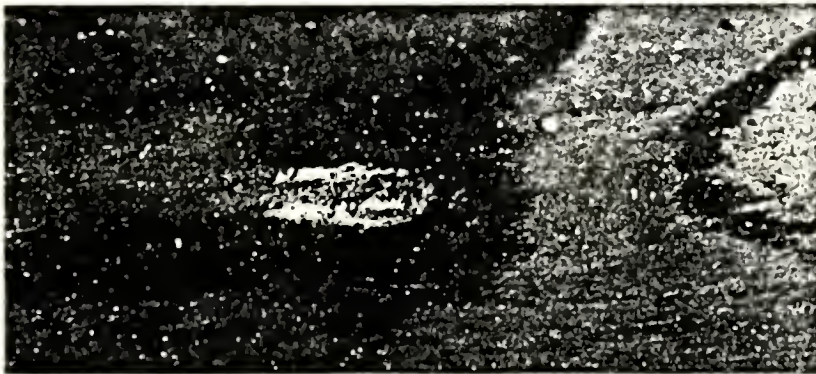


FLOW  
←

FIG. 17

40 X

SALT  
SULFIDE

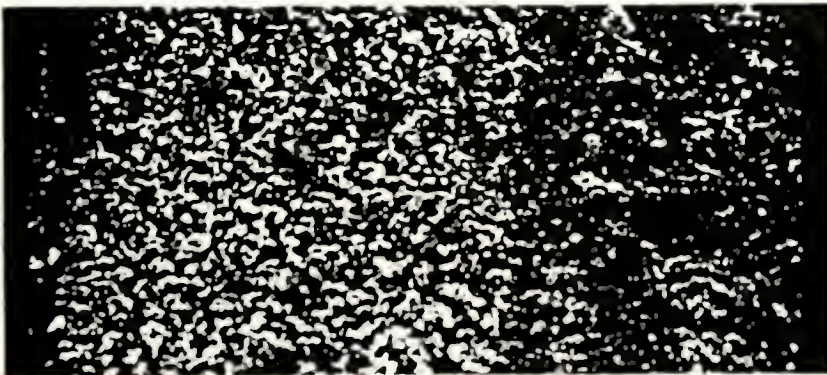


FLOW  
←

FIG. 18

40 X

SALT  
SULFIDE



DARK  
FILM

FIG. 19

1000 X



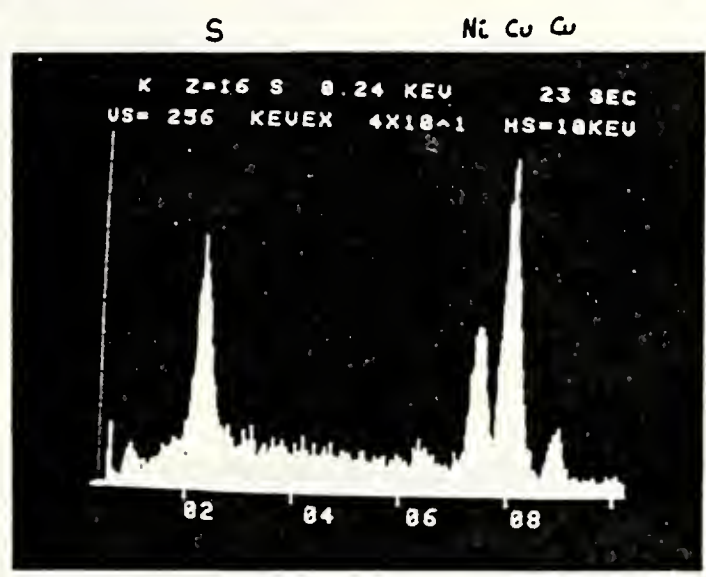


FIG. 20

SALT  
SULFIDE



FIG. 21

100 X





FIG. 22 1000 X



FIG. 23 100 X

SULFUR

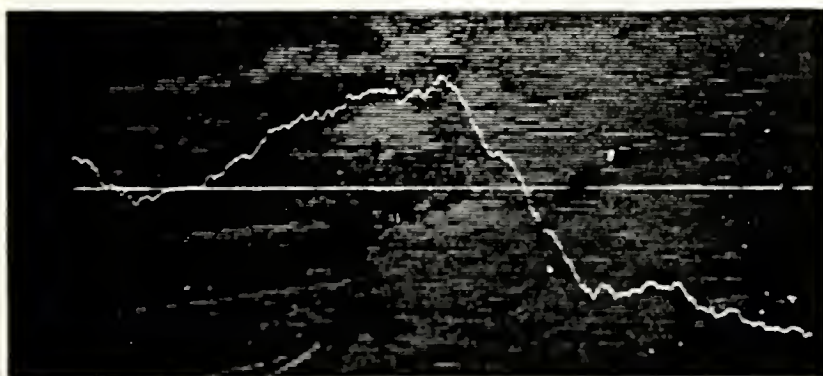


FIG. 24



COPPER

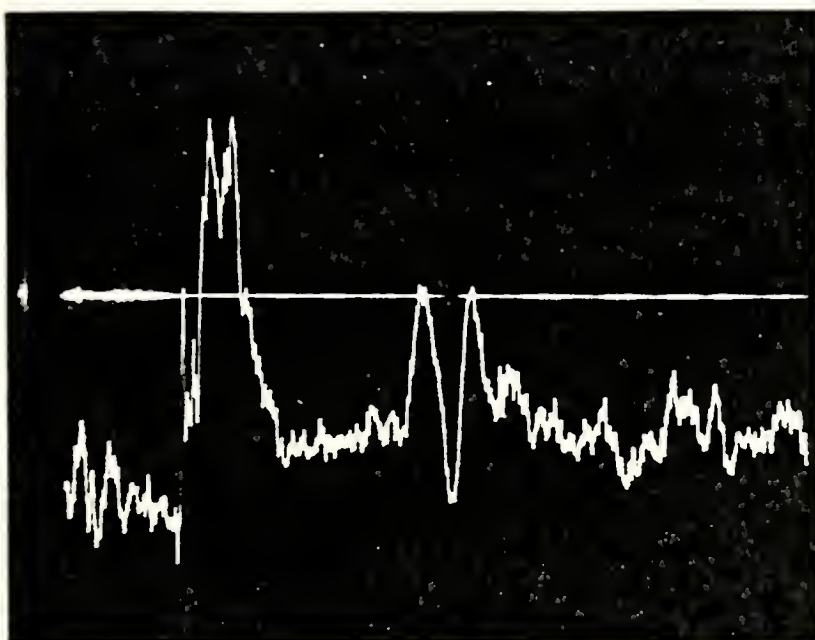


FIG. 25

NICKEL

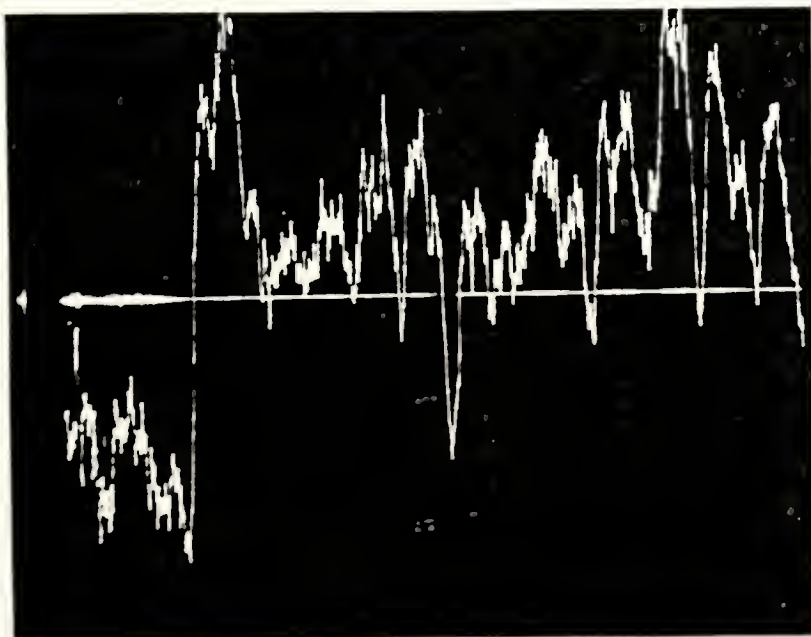
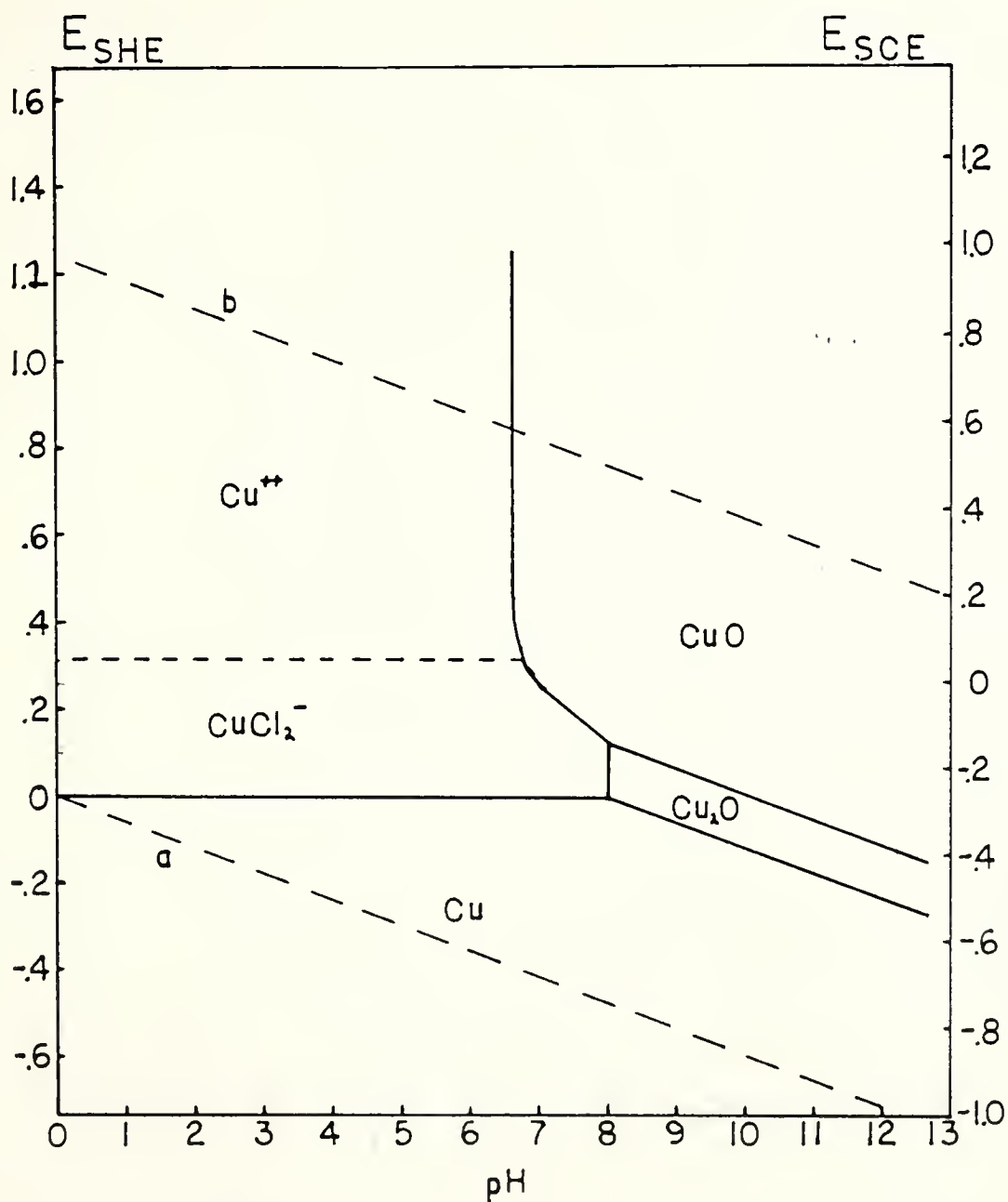


FIG. 26

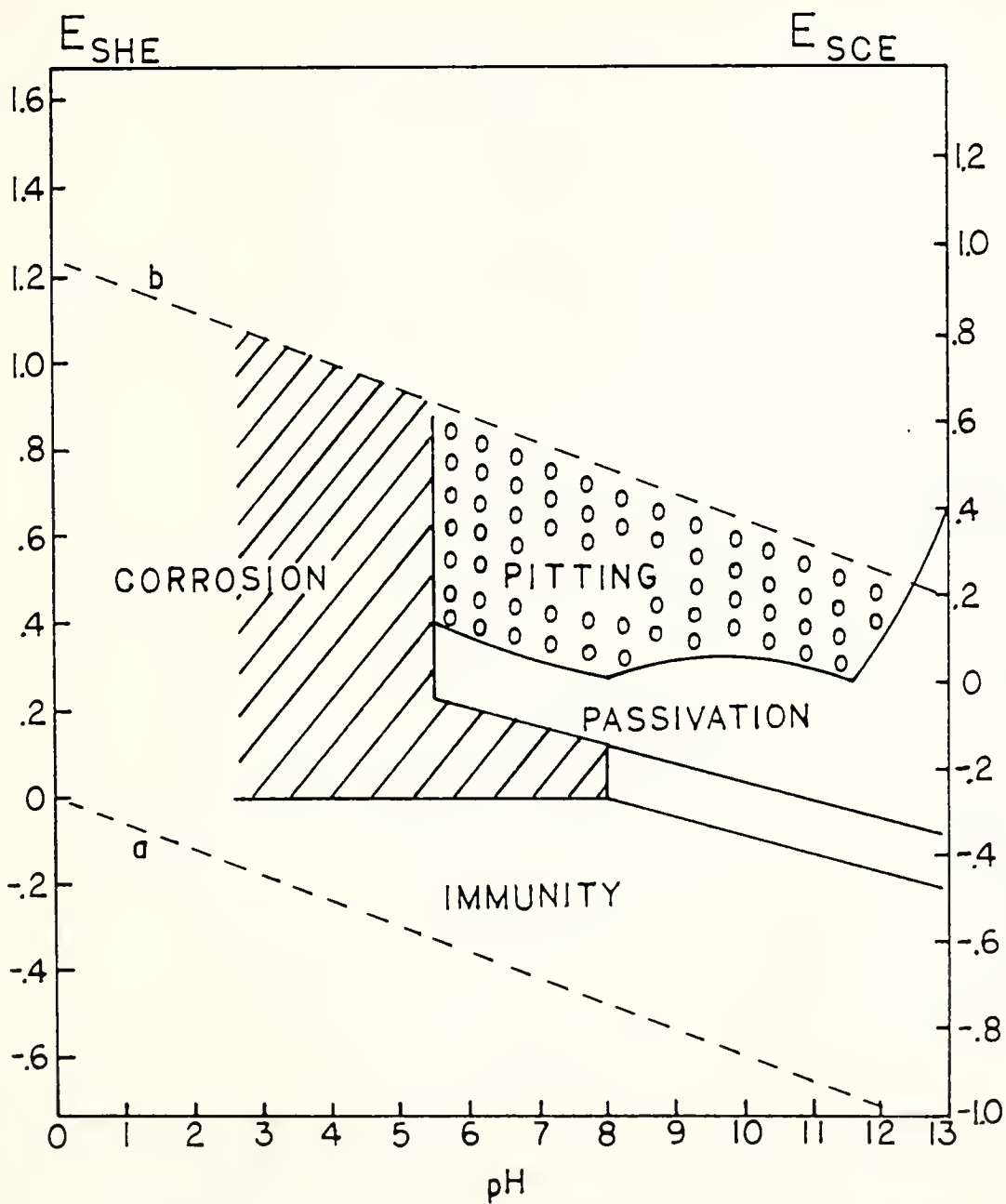




POURBAIX DIAGRAM FOR PURE COPPER

FIG.27

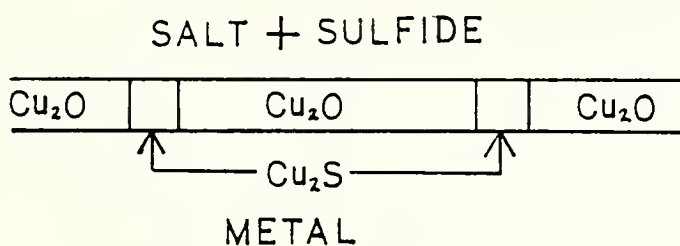




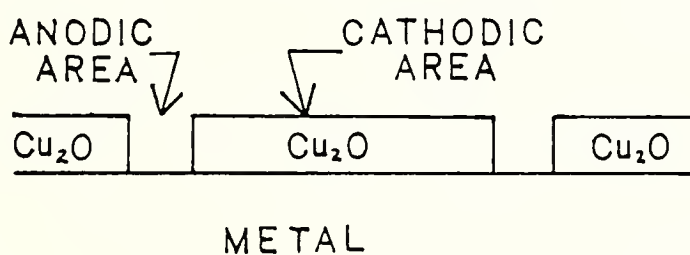
EXPERIMENTAL POTENTIAL-PH DIAGRAM  
FOR 70-30 CUPRONICKEL

FIG. 28

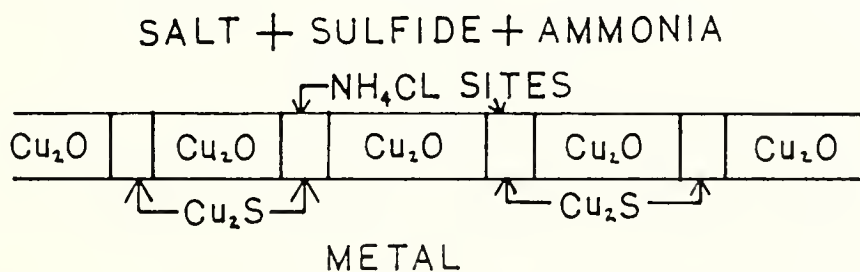




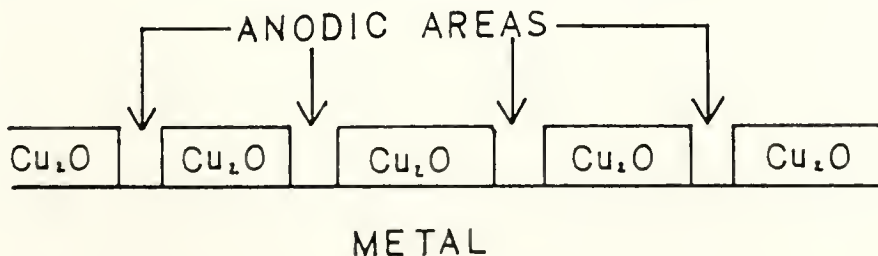
29-A



29-B



29-C



29-D

FIG. 29







Thesis  
B819  
c.1

Brown

190641

Investigation of the  
accelerated corrosion  
of cupro-nickel piping.

Thesis  
B819  
c.1

Brown

190641

Investigation of the  
accelerated corrosion  
of cupro-nickel piping.

thesB819

Investigation of the accelerated corrosi



3 2768 002 08017 8

DUDLEY KNOX LIBRARY